Available online at www.sciencedirect.com
SCIENCE DIRECT®
International Journal of Solids and Structures 42 (2005) 2851–2882
INTERNATIONAL JOURNAL OF SOLIDS and STRUCTURES
www.elsevier.com/locate/ijsolstr

# Non-canonical Minkowski and pseudo-Riemann frames of plasticity models with anisotropic quadratic yield criteria

Chein-Shan Liu [a,*], Chih-Wen Chang [b]

[a] Department of Mechanical and Mechatronic Engineering, National Taiwan Ocean University, Keelung 20224, Taiwan
[b] Department of System Engineering and Naval Architecture, National Taiwan Ocean University, Keelung, Taiwan

Received 1 April 2004; received in revised form 18 September 2004
Available online 2 November 2004

**Abstract**

Including the von Mises, the Drucker–Prager and the Hill there are many material plastic models with the yield criteria based on the quadratic yield functions. In this paper we study the associated plastic flow model with an anisotropic yield criterion $\boldsymbol{\sigma}^{\mathrm{t}}\mathbf{C}^{-1}\boldsymbol{\sigma}+2\mathbf{V}^{\mathrm{t}}\boldsymbol{\sigma}=2S_y$, where $\boldsymbol{\sigma}$ is a suitable stress vector and $\mathbf{V}$ reflects the asymmetric yield strength in tension and compression, and with an anisotropic elastic law $\dot{\boldsymbol{\sigma}}=\mathbf{K}\dot{\boldsymbol{\varepsilon}}$ in the elastic phase. We first consider the term $\boldsymbol{\sigma}^{\mathrm{t}}\mathbf{C}^{-1}\boldsymbol{\sigma}$ to be a strain-energy, which means that the anisotropic tensor $\mathbf{C}$ is positive definite and coincides with the elastic tensor $\mathbf{K}$. Under this additional assumption, we can prove that the governing equations of plasticity can be linearized in a non-canonical Minkowski space. The internal symmetry of the plastic equation is a special orthochronous pseudo-linear group $\mathrm{SL}(n,1,\mathbb{R})$. A further variable transformation reveals a canonical Minkowski structure, of which the plastic equation exhibits the proper orthochronous Lorentz group symmetry $\mathrm{SO}_{\mathrm{o}}(n,1)$.

Then, we release the constraint by allowing the above $\mathbf{C}^{-1}$ to be free, which may be positive, non-positive or even singular. For this case the plastic equation becomes highly non-linear. We approach this problem by converting the non-linear constitutive equations to a Lie system $\dot{\mathbf{X}}=\mathbf{A}(\mathbf{X},t)\mathbf{X}$ on a pseudo-Riemann manifold, where $\mathbf{A}\in\mathrm{sl}(n,1,\mathbb{R})$ is a real Lie algebra of the special orthochronous pseudo-linear group $\mathrm{SL}(n,1,\mathbb{R})$. The underlying space in the plastic phase is a cone with the metric tensor indefinite having a signature $(n,1)$ and also dependent on the temporal component. Based on these symmetry groups the exact solutions or the Cayley transform are developed, which can update the stress point exactly on the yield surface at every time increment without any iteration. As numerical examples, we calculate the stress responses for the Drucker–Prager and Hill models.


*Keywords:* Elastoplasticity; Quadratic yield criterion; Non-canonical Minkowski space; Pseudo-Riemann manifold; Symmetry group; Lorentz group; Pseudo-linear group

* Corresponding author. Tel.: +886 2 2462 2192x3252; fax: +886 2 2462 0836.
*E-mail address:* csliu@mail.ntou.edu.tw (C.-S. Liu).

0020-7683/$ - see front matter © 2004 Elsevier Ltd. All rights reserved.
doi:10.1016/j.ijsolstr.2004.09.035

## 1. Introduction

In the study of engineering mechanical problems a substantial role is played by the constitutive relations of elastoplasticity, to which many theoretical, computational and experimental contributions have been made. To characterize the elastoplastic behavior of materials an important concept is the yield criterion, which defines the elastic limit of a material under combined states of stress. For a pressure independent material, the most widely used is the von Mises yield criterion:

$$s_{ij}s_{ij} = 2\tau_y^2, \tag{1}$$

where

$$s_{ij} = \sigma_{ij} - \tfrac{1}{3}\sigma_{kk}\delta_{ij} \tag{2}$$

is the deviatoric components of stress $\sigma_{ij}$, and $\tau_y$ is the shear yield strength. In terms of $\sigma_{ij}$, the yield criterion (1) can also be expressed as

$$(\sigma_{11}-\sigma_{22})^2 + (\sigma_{22}-\sigma_{33})^2 + (\sigma_{33}-\sigma_{11})^2 + 6(\sigma_{12}^2+\sigma_{13}^2+\sigma_{23}^2) = 6\tau_y^2. \tag{3}$$

In the stress space, the above yield surface is symmetric to the zero stress point, and therefore is only applicable to the isotropic materials, which do not need the directional requirement to describe the deformation behavior. However, for the anisotropic sheet metals the deformed property is directional with respect to the rolling direction of sheet plane, which in turn requires that the yield function does not only deal with the directions of stress components but also involves the directional deformation behavior. A yield criterion to describe the orthotropic behavior is first proposed by Hill (1948). An orthotropic material has three orthogonal planes of material symmetry. The intersection of these planes are the principal axes of anisotropy. Hill's yield criterion when referred to these axes has the following form:

$$F(\sigma_{22}-\sigma_{33})^2 + G(\sigma_{33}-\sigma_{11})^2 + H(\sigma_{11}-\sigma_{22})^2 + 2L\sigma_{23}^2 + 2M\sigma_{13}^2 + 2N\sigma_{12}^2 = 1, \tag{4}$$

where $F, G, \ldots, N$ are material constants of the current state of anisotropy.

Eq. (4) is a quadratic function of stress components, representing some kind of energy that governs the yielding behavior of orthotropic materials. Hill's yield criterion is an extension of the distortion energy criterion of von Mises. However, the omission of the linear terms and the appearance of only differences between normal stress components in the yield criteria (3) and (4) imply the assumptions that the material responses are equal in tension and compression and that the pressure does not influence the yielding behavior.

Despite that there are many materials whose yielding behaviors are pressure sensitive and different in tensile and compressive loadings. For example, a wide range of geotechnical materials including rock, concrete, and soil display a pressure-dependent yielding behavior and an inelastic volumetric dilatancy. About these materials the Drucker and Prager (1952) yield criterion reflects such dependence on pressure:

$$(\sigma_{11}-\sigma_{22})^2 + (\sigma_{22}-\sigma_{33})^2 + (\sigma_{33}-\sigma_{11})^2 + 6(\sigma_{12}^2+\sigma_{13}^2+\sigma_{23}^2) = 6[\tau_y - \alpha(\sigma_{11}+\sigma_{22}+\sigma_{33})]^2, \tag{5}$$

where $\tau_y$ is once again the shear yield strength, and $\alpha$ is the frictional coefficient of material quantifying the effect of hydrostatic pressure.

Ice is a columnar-grained crystal, which may be treated as an orthotropic material. However, as pointed out by Reinicke and Ralston (1977) the strength of ice is sensitive to the hydrostatic pressure. Its tensile strength is much smaller than its compressive strength. A modification of Hill's yield criterion is thus proposed by Reinicke and Ralston (1977):

$$F[(\sigma_{22}-\sigma_{33})^2+(\sigma_{33}-\sigma_{11})^2]+H(\sigma_{11}-\sigma_{22})^2+2L[\sigma_{23}^2+\sigma_{13}^2]+2(F+2H)\sigma_{12}^2+P(\sigma_{11}+\sigma_{22})+Q\sigma_{33}=1. \tag{6}$$

Eqs. (5) and (6) both including the linear terms of normal stresses, describe materials with different tensile and compressive strengths and predict a non-linear increase in shear strength with a confining pressure. Motivated by Hill's yield criterion and the results for solids with different tensile and compressive yield stresses, Liu et al. (1997) have proposed the following yield criterion:

$$F(\sigma_{22}-\sigma_{33})^2+G(\sigma_{33}-\sigma_{11})^2+H(\sigma_{11}-\sigma_{22})^2+2L\sigma_{23}^2+2M\sigma_{13}^2+2N\sigma_{12}^2=[I\sigma_{11}+J\sigma_{22}+K\sigma_{33}-1]^2, \tag{7}$$

and derived the formulae to determine these coefficients through the uniaxial tension–compression and simple shearing tests.

In this paper we are going to study the internal symmetry groups, the underlying spaces of the associated flow models and the consistent numerical schemes with the following quadratic yield criterion in the plastic phase:

$$\boldsymbol{\sigma}^{\mathrm{t}}\mathbf{C}^{-1}\boldsymbol{\sigma}+2\mathbf{V}^{\mathrm{t}}\boldsymbol{\sigma}=2S_y, \tag{8}$$

together with the rate equation

$$\dot{\boldsymbol{\sigma}}=\mathbf{K}\dot{\boldsymbol{\varepsilon}} \tag{9}$$

in the elastic phase with its $\mathbf{K}$ positive definite. Here $\boldsymbol{\sigma}$ is a suitable stress vector. Throughout this paper a superimposed dot is a material time derivative, and a superscript t denotes the transpose.

As that done by Oller et al. (2003), it is not difficult to prove that the yield criteria (3)–(7) are all special cases of Eq. (8), corresponding to different anisotropic tensor $\mathbf{C}^{-1}$, eccentric vector $\mathbf{V}$ and material constant $S_y$. The followings correspond to the yield criterion of Drucker and Prager (1952):

$$\mathbf{C}^{-1}=\begin{bmatrix} 1-3\alpha^2 & \frac{-1}{2}-3\alpha^2 & \frac{-1}{2}-3\alpha^2 & 0 & 0 & 0\\ \frac{-1}{2}-3\alpha^2 & 1-3\alpha^2 & \frac{-1}{2}-3\alpha^2 & 0 & 0 & 0\\ \frac{-1}{2}-3\alpha^2 & \frac{-1}{2}-3\alpha^2 & 1-3\alpha^2 & 0 & 0 & 0\\ 0 & 0 & 0 & 3 & 0 & 0\\ 0 & 0 & 0 & 0 & 3 & 0\\ 0 & 0 & 0 & 0 & 0 & 3 \end{bmatrix}, \qquad \mathbf{V}=3\tau_y\alpha\begin{bmatrix}1\\1\\1\\0\\0\\0\end{bmatrix}, \tag{10}$$

and $S_y=3\tau_y^2/2$. The followings correspond to the yield criterion of Hill (1948):

$$\mathbf{C}^{-1}=\begin{bmatrix} H+G & -H & -G & 0 & 0 & 0\\ -H & H+F & -F & 0 & 0 & 0\\ -G & -F & F+G & 0 & 0 & 0\\ 0 & 0 & 0 & 2L & 0 & 0\\ 0 & 0 & 0 & 0 & 2M & 0\\ 0 & 0 & 0 & 0 & 0 & 2N \end{bmatrix}, \qquad \mathbf{V}=\mathbf{0}, \tag{11}$$

and $S_y = 1/2$. The followings correspond to the yield criterion of Reinicke and Ralston (1977):

$$\mathbf{C}^{-1} = \begin{bmatrix} H+F & -H & -F & 0 & 0 & 0 \\ -H & H+F & -F & 0 & 0 & 0 \\ -F & -F & 2F & 0 & 0 & 0 \\ 0 & 0 & 0 & 2L & 0 & 0 \\ 0 & 0 & 0 & 0 & 2L & 0 \\ 0 & 0 & 0 & 0 & 0 & 2(F+2H) \end{bmatrix}, \qquad \mathbf{V} = \begin{bmatrix} \frac{P}{2} \\ \frac{P}{2} \\ \frac{Q}{2} \\ 0 \\ 0 \\ 0 \end{bmatrix}, \tag{12}$$

and $S_y = 1/2$. And, the followings correspond to the yield criterion of Liu et al. (1997):

$$\mathbf{C}^{-1} = \begin{bmatrix} H+G-I^2 & -H-IJ & -G-IK & 0 & 0 & 0 \\ -H-IJ & H+F-J^2 & -F-JK & 0 & 0 & 0 \\ -G-IK & -F-JK & F+G-K^2 & 0 & 0 & 0 \\ 0 & 0 & 0 & 2L & 0 & 0 \\ 0 & 0 & 0 & 0 & 2M & 0 \\ 0 & 0 & 0 & 0 & 0 & 2N \end{bmatrix}, \qquad \mathbf{V} = \begin{bmatrix} I \\ J \\ K \\ 0 \\ 0 \\ 0 \end{bmatrix}, \tag{13}$$

and $S_y = 1/2$.

Let us investigate the property of $\mathbf{C}^{-1}$. For the von Mises yield criterion (3) we have

$$\mathbf{C}^{-1} = \begin{bmatrix} 2 & -1 & -1 & 0 & 0 & 0 \\ -1 & 2 & -1 & 0 & 0 & 0 \\ -1 & -1 & 2 & 0 & 0 & 0 \\ 0 & 0 & 0 & 6 & 0 & 0 \\ 0 & 0 & 0 & 0 & 6 & 0 \\ 0 & 0 & 0 & 0 & 0 & 6 \end{bmatrix}, \qquad \boldsymbol{\sigma} = \begin{bmatrix} \sigma_{11} \\ \sigma_{22} \\ \sigma_{33} \\ \sigma_{23} \\ \sigma_{13} \\ \sigma_{12} \end{bmatrix}. \tag{14}$$

The above $\mathbf{C}^{-1}$ is singular and non-negative definite because the eigenvalues of $\mathbf{C}^{-1}$ are 0, 3 (double) and 6 (triple).

The von Mises yield criterion (1) can also be expressed in another two forms due to $s_{11} + s_{22} + s_{33} = 0$:

$$s_{11}^2 + s_{22}^2 + s_{11}s_{22} + s_{23}^2 + s_{13}^2 + s_{12}^2 = \tau_y^2, \tag{15}$$

$$-s_{11}s_{22} - s_{22}s_{33} - s_{33}s_{11} + s_{23}^2 + s_{13}^2 + s_{12}^2 = \tau_y^2. \tag{16}$$

For Eq. (15) we have

$$\mathbf{C}^{-1} = \begin{bmatrix} 1 & \frac{1}{2} & 0 & 0 & 0 \\ \frac{1}{2} & 1 & 0 & 0 & 0 \\ 0 & 0 & 1 & 0 & 0 \\ 0 & 0 & 0 & 1 & 0 \\ 0 & 0 & 0 & 0 & 1 \end{bmatrix}, \qquad \boldsymbol{\sigma} = \begin{bmatrix} s_{11} \\ s_{22} \\ s_{23} \\ s_{13} \\ s_{12} \end{bmatrix}. \tag{17}$$

Obviously, the above $\mathbf{C}^{-1}$ is positive definite. But for Eq. (16) we have

$$\mathbf{C}^{-1}=\begin{bmatrix} 0 & -\frac{1}{2} & -\frac{1}{2} & 0 & 0 & 0 \\ -\frac{1}{2} & 0 & -\frac{1}{2} & 0 & 0 & 0 \\ -\frac{1}{2} & -\frac{1}{2} & 0 & 0 & 0 & 0 \\ 0 & 0 & 0 & 1 & 0 & 0 \\ 0 & 0 & 0 & 0 & 1 & 0 \\ 0 & 0 & 0 & 0 & 0 & 1 \end{bmatrix}, \qquad \boldsymbol{\sigma}=\begin{bmatrix} s_{11} \\ s_{22} \\ s_{33} \\ s_{23} \\ s_{13} \\ s_{12} \end{bmatrix}, \tag{18}$$

where $\mathbf{C}^{-1}$ is not positive definite, because its eigenvalues are $-1$, 1/2 (double) and 1 (triple).

Even for the same yield criterion of von Mises, the above analyses indicate that representing the yield criterion in different stress spaces may lead to different properties of $\mathbf{C}^{-1}$. The best choice seems Eq. (15) due to its lower dimension and the positive definiteness of $\mathbf{C}^{-1}$. Two another non-positive examples are the Drucker–Prager yield criterion, whose $\mathbf{C}^{-1}$ as given in Eq. (10) has eigenvalues $-9\alpha^2$, 3/2 (double) and 3 (triple), and the Hill yield criterion, whose $\mathbf{C}^{-1}$ as given in Eq. (11) has eigenvalues 0, $2L$, $2M$, $2N$ and $F+G+H-(F^2+G^2+H^2-FG-FH-GH)^{1/2}$ (double). Especially, the latter $\mathbf{C}^{-1}$ is a singular matrix.

In Section 2 we use the concept of strain energy to construct the asymmetric yield criterion (8) by restricting $\mathbf{C}=\mathbf{K}$ to be positive definite and call it a strain-energy yielding model; otherwise, when $\mathbf{K}\neq\mathbf{C}$ we call it an anisotropic quadratic yielding model. For the strain-energy elastoplastic flow model specified in Section 3 we derive an on–off switch in Section 4, where the non-linearity of the plastic equation is shown. Even the plastic equation is non-linear in the stress space we can transform it to a linear system in a non-canonical Minkowski space in Section 5. Then, we further reduce the non-canonical linear system to a canonical one in Section 6. In Section 7 we solve the numerical integration problems of the flow model under strain and stress controls by employing a group-theoretic approach. For the elastoplastic flow model with a non-positive $\mathbf{C}^{-1}$ (including the Drucker–Prager model and the Hill model) and with the elastic law (9) the investigation of its internal symmetry properties will be conducted in Sections 8 and 9.

## 2. Strain-energy yield criterion

The generalized Hooke's law is

$$\sigma_{\alpha\beta}=K_{\alpha\beta\gamma\delta}\varepsilon_{\gamma\delta}, \quad \alpha,\beta,\gamma,\delta=1,2,3. \tag{19}$$

Because $\alpha$, $\beta$, $\gamma$, $\delta$ take values over 1, 2, 3, there are $3^4=81$ material constants for $K_{\alpha\beta\gamma\delta}$. However, because of $\varepsilon_{\gamma\delta}=\varepsilon_{\delta\gamma}$ by the definition of small strain, Eq. (19) yields the result that $K_{\alpha\beta\gamma\delta}=K_{\alpha\beta\delta\gamma}$. Also, for the non-polar materials the stress tensor is symmetric, i.e., $\sigma_{\alpha\beta}=\sigma_{\beta\alpha}$, and therefore $K_{\alpha\beta\gamma\delta}=K_{\beta\alpha\gamma\delta}$. Consequently, we have

$$K_{\alpha\beta\gamma\delta}=K_{\beta\alpha\gamma\delta}, \qquad K_{\alpha\beta\gamma\delta}=K_{\alpha\beta\delta\gamma}. \tag{20}$$

Observing the symmetries exist between the two pairs of indices $(\alpha,\beta)$ and $(\gamma,\delta)$, we have 36 independent elastic constants for $K_{\alpha\beta\gamma\delta}$.

If we consider an infinitesimal volume element, the strain energy per unit volume can be written as:

$$\delta U=\sigma_{\alpha\beta}\delta\varepsilon_{\alpha\beta}, \tag{21}$$

where $U$ is a function of the strain components $\varepsilon_{\alpha\beta}$. Accordingly, if $U=\sigma_{\alpha\beta}\varepsilon_{\alpha\beta}/2=K_{\alpha\beta\gamma\delta}\varepsilon_{\alpha\beta}\varepsilon_{\gamma\delta}/2$ is written symmetrically in terms of the strain components $\varepsilon_{\alpha\beta}$, Eq. (21) yields

$$\frac{\partial U}{\partial\varepsilon_{\alpha\beta}}\delta\varepsilon_{\alpha\beta}=\sigma_{\alpha\beta}\delta\varepsilon_{\alpha\beta}, \tag{22}$$

and thus,

$$\sigma_{\alpha\beta} = \frac{\partial U}{\partial \varepsilon_{\alpha\beta}}. \tag{23}$$

Accordingly, Eqs. (19) and (23) together with

$$\frac{\partial^2 U}{\partial \varepsilon_{\alpha\beta}\partial \varepsilon_{\gamma\delta}} = \frac{\partial^2 U}{\partial \varepsilon_{\gamma\delta}\partial \varepsilon_{\alpha\beta}}, \tag{24}$$

lead to

$$K_{\alpha\beta\gamma\delta} = K_{\gamma\delta\alpha\beta}. \tag{25}$$

Consequently, the symmetries of strain and stress tensors together with the postulated energy function lead to the usual symmetries of the elastic tensor:

$$K_{\alpha\beta\gamma\delta} = K_{\beta\alpha\gamma\delta} = K_{\alpha\beta\delta\gamma} = K_{\gamma\delta\alpha\beta}. \tag{26}$$

For its most general case there are 21 independent components of $K_{\alpha\beta\gamma\delta}$.

Under the correspondences $\sigma_{11} \leftrightarrow \sigma_1$, $\sigma_{22} \leftrightarrow \sigma_2$, $\sigma_{33} \leftrightarrow \sigma_3$, $\sigma_{23} \leftrightarrow \sigma_4$, $\sigma_{13} \leftrightarrow \sigma_5$, $\sigma_{12} \leftrightarrow \sigma_6$, $\varepsilon_{11} \leftrightarrow \varepsilon_1$, $\varepsilon_{22} \leftrightarrow \varepsilon_2$, $\varepsilon_{33} \leftrightarrow \varepsilon_3$, $\varepsilon_{23} \leftrightarrow \varepsilon_4$, $\varepsilon_{13} \leftrightarrow \varepsilon_5$, $\varepsilon_{12} \leftrightarrow \varepsilon_6$, and for the convenient manipulation we may convert the tensor form (19) into the vector form by the above arguments of symmetry:

$$\begin{bmatrix} \sigma_1 \\ \sigma_2 \\ \sigma_3 \\ \sigma_4 \\ \sigma_5 \\ \sigma_6 \end{bmatrix} = \begin{bmatrix} K_{11} & K_{12} & K_{13} & K_{14} & K_{15} & K_{16} \\ & K_{22} & K_{23} & K_{24} & K_{25} & K_{26} \\ & & K_{33} & K_{34} & K_{35} & K_{36} \\ & & & K_{44} & K_{45} & K_{46} \\ & \text{Sym.} & & & K_{55} & K_{56} \\ & & & & & K_{66} \end{bmatrix} \begin{bmatrix} \varepsilon_1 \\ \varepsilon_2 \\ \varepsilon_3 \\ \varepsilon_4 \\ \varepsilon_5 \\ \varepsilon_6 \end{bmatrix}. \tag{27}$$

In terms of the stress vector $\boldsymbol{\sigma}$ the elastic strain energy can be written as

$$U = \tfrac{1}{2}\boldsymbol{\sigma}^{\mathrm{t}}\mathbf{K}^{-1}\boldsymbol{\sigma}. \tag{28}$$

Motivated by the strain energy and the results for solids with different tensile and compressive yield stresses, we consider the following quadratic yield criterion:

$$2U + 2\mathbf{V}^{\mathrm{t}}\boldsymbol{\sigma} = \boldsymbol{\sigma}^{\mathrm{t}}\mathbf{K}^{-1}\boldsymbol{\sigma} + 2\mathbf{V}^{\mathrm{t}}\boldsymbol{\sigma} = 2S_y. \tag{29}$$

The basic requirement of this strain-energy based model is the positive definiteness of $\mathbf{K}^{-1}$. In addition $\mathbf{K}^{-1}$ we should determine $S_y$ and $\mathbf{V}$ for the modeled materials. For example, the von Mises yield criterion (1) can be written as

$$\frac{1}{2\mu}s_{ij}s_{ij} = \frac{\tau_y^2}{\mu} \tag{30}$$

with $\mathbf{K}^{-1} = \mathbf{I}_6/(2\mu)$ positive definite, $S_y = \tau_y^2/(2\mu)$ and $\mathbf{V} = \mathbf{0}$ in Eq. (29), where $\mu$ is the shear modulus of the isotropic material. Because of $s_{11} + s_{22} + s_{33} = 0$, it can also be written as

$$\frac{1}{2\mu}[s_{11}^2 + s_{22}^2 + s_{11}s_{22} + s_{23}^2 + s_{13}^2 + s_{12}^2] = \frac{\tau_y^2}{2\mu}, \tag{31}$$

from which we have

$$\mathbf{K}^{-1}=\begin{bmatrix} \frac{1}{2\mu} & \frac{1}{4\mu} & 0 & 0 & 0 \\ \frac{1}{4\mu} & \frac{1}{2\mu} & 0 & 0 & 0 \\ 0 & 0 & \frac{1}{2\mu} & 0 & 0 \\ 0 & 0 & 0 & \frac{1}{2\mu} & 0 \\ 0 & 0 & 0 & 0 & \frac{1}{2\mu} \end{bmatrix}, \qquad \boldsymbol{\sigma}=\begin{bmatrix} s_{11} \\ s_{22} \\ s_{23} \\ s_{13} \\ s_{12} \end{bmatrix}. \tag{32}$$

The above $\mathbf{K}^{-1}$ is also positive definite.

In Sections 3–7 we investigate the plastic flow properties for positive $\mathbf{K}^{-1}$ in a suitable stress–strain space. For example, for materials with the von Mises yield criterion, we can treat the flow model with the yield criterion (31) and with the following anisotropic elastic law:

$$\begin{bmatrix} s_{11} \\ s_{22} \\ s_{23} \\ s_{13} \\ s_{12} \end{bmatrix}=\begin{bmatrix} \frac{8\mu}{3} & -\frac{4\mu}{3} & 0 & 0 & 0 \\ -\frac{4\mu}{3} & \frac{8\mu}{3} & 0 & 0 & 0 \\ 0 & 0 & 2\mu & 0 & 0 \\ 0 & 0 & 0 & 2\mu & 0 \\ 0 & 0 & 0 & 0 & 2\mu \end{bmatrix}\begin{bmatrix} e_{11} \\ e_{22} \\ e_{23} \\ e_{13} \\ e_{12} \end{bmatrix} \tag{33}$$

in the deviatoric stress and strain spaces.

## 3. The flow model with strain energy as a yield criterion

Now, let us consider the following flow model:

$$\dot{\boldsymbol{\varepsilon}}=\dot{\boldsymbol{\varepsilon}}^{e}+\dot{\boldsymbol{\varepsilon}}^{p}, \tag{34}$$

$$\mathbf{K}^{-1}\dot{\boldsymbol{\sigma}}=\dot{\boldsymbol{\varepsilon}}^{e}, \tag{35}$$

$$(\mathbf{K}^{-1}\boldsymbol{\sigma}+\mathbf{V})\dot{\lambda}=\dot{\boldsymbol{\varepsilon}}^{p}, \tag{36}$$

$$f(\boldsymbol{\sigma})\leqslant 0, \tag{37}$$

$$\dot{\lambda}\geqslant 0, \tag{38}$$

$$\dot{\lambda}f(\boldsymbol{\sigma})=0. \tag{39}$$

Depending on the number of non-zero stress components in above (and correspondingly the non-zero strain components) which we consider for a physical problem, for example, the axial tension–compression problem, the biaxial tension–compression–torsion problem, etc., the dimensions $n$ may be an integer with $1\leqslant n\leqslant 6$, and no matter which case we use $n$ to denote the physical problem dimensions. In the above, $\mathbf{K}$ is of order $n\times n$, symmetric and positive definite; $\mathbf{V}$ is of order $n$; and $S_y$ is a positive scalar. As can be seen, $\mathbf{K}^{-1}$, $\mathbf{V}$ and $S_y$ are the coefficients of the yield function

$$f(\boldsymbol{\sigma})=\boldsymbol{\sigma}^{\mathrm{t}}\mathbf{K}^{-1}\boldsymbol{\sigma}+2\mathbf{V}^{\mathrm{t}}\boldsymbol{\sigma}-2S_y \tag{40}$$

as defined in Eq. (29). $\mathbf{K}^{-1}$ is the compliance matrix; $\mathbf{V}$ is the eccentric point vector reflecting the asymmetry of the yield surface in stress space; and $S_y$ is a specific strain energy at the yielding state. The yielding criterion (29) is an extension of the strain-energy criterion by including the term of $\mathbf{V}$, which accounts of the effect of residual stress on the yielding behavior.

A novel formulation for the elastoplasticity with the von Mises yield criterion (30) has been developed by Hong and Liu (1999a,b, 2000), Liu and Hong (2000, 2001), Mukherjee and Liu (2003), and Liu (2001a, 2003a, 2004a,b). Then, Liu (2004c) and Liu and Chang (2004) extended these studies to the Drucker–Prager model and convex plastic model. These authors explored the internal symmetry groups in the Minkowski space of the constitutive models of perfect elastoplasticity with or without considering large deformation, bilinear elastoplasticity, visco-elastoplasticity, isotropic work-hardening elastoplasticity, mixed-hardening elastoplasticity, the Drucker–Prager plasticity model as well as a rather general flow model with the yield function convex to ensure that the consistency condition is exactly satisfied at each time step once the computational schemes can take these symmetries into account.

The models considered so far are all isotropic ones except the Drucker–Prager model and convex plastic model. To construct an anisotropic model, recalling that the Minkowski space $\mathbb{M}^{n+1}$ is a pseudo-Euclidean space (with rank $n+1$ and index $n$), we need only to generalize the pseudo-Euclidean space to a pseudo-Riemannian space by specifying a non-canonical metric tensor:

$$\mathscr{G} := \begin{bmatrix} \mathbf{K}^{-1} & \mathbf{V} \\ \mathbf{V}^{\mathrm{t}} & -2S_y \end{bmatrix},$$

where $\mathbf{K}$, $\mathbf{V}$ and $S_y$ are used in the yield criterion (29). Note that in this generalization the inertia (namely, the rank and the numbers of positive and negative eigenvalues) of the metric tensor remains unchanged (compare the above metric with the canonical metric tensor (71) to be appeared in Section 6). As a consequence we can embed the anisotropic strain-energy yielding flow model into an augmented linear system in the non-canonical Minkowski space.

## 4. Switch for the mechanism of plasticity

Substituting Eqs. (35) and (36) into Eq. (34) gives

$$\mathbf{K}^{-1}\dot{\boldsymbol{\sigma}} + (\mathbf{K}^{-1}\boldsymbol{\sigma} + \mathbf{V})\dot{\lambda} = \dot{\boldsymbol{\varepsilon}}, \tag{41}$$

which being taken inner product with $\boldsymbol{\sigma}$ and with $\mathbf{KV}$ respectively, lead to

$$\boldsymbol{\sigma}^{\mathrm{t}}\mathbf{K}^{-1}\dot{\boldsymbol{\sigma}} + (\boldsymbol{\sigma}^{\mathrm{t}}\mathbf{K}^{-1}\boldsymbol{\sigma} + \mathbf{V}^{\mathrm{t}}\boldsymbol{\sigma})\dot{\lambda} = \boldsymbol{\sigma}^{\mathrm{t}}\dot{\boldsymbol{\varepsilon}}, \tag{42}$$

$$\mathbf{V}^{\mathrm{t}}\dot{\boldsymbol{\sigma}} + (\mathbf{V}^{\mathrm{t}}\boldsymbol{\sigma} + \mathbf{V}^{\mathrm{t}}\mathbf{K}\mathbf{V})\dot{\lambda} = \mathbf{V}^{\mathrm{t}}\mathbf{K}\dot{\boldsymbol{\varepsilon}}. \tag{43}$$

The sum of Eqs. (42) and (43) gives

$$\boldsymbol{\sigma}^{\mathrm{t}}\mathbf{K}^{-1}\dot{\boldsymbol{\sigma}} + \mathbf{V}^{\mathrm{t}}\dot{\boldsymbol{\sigma}} + (\boldsymbol{\sigma}^{\mathrm{t}}\mathbf{K}^{-1}\boldsymbol{\sigma} + 2\mathbf{V}^{\mathrm{t}}\boldsymbol{\sigma} + \mathbf{V}^{\mathrm{t}}\mathbf{K}\mathbf{V})\dot{\lambda} = \boldsymbol{\sigma}^{\mathrm{t}}\dot{\boldsymbol{\varepsilon}} + \mathbf{V}^{\mathrm{t}}\mathbf{K}\dot{\boldsymbol{\varepsilon}}. \tag{44}$$

When the yield condition and consistency condition

$$\boldsymbol{\sigma}^{\mathrm{t}}\mathbf{K}^{-1}\boldsymbol{\sigma} + 2\mathbf{V}^{\mathrm{t}}\boldsymbol{\sigma} = 2S_y, \tag{45}$$

$$\boldsymbol{\sigma}^{\mathrm{t}}\mathbf{K}^{-1}\dot{\boldsymbol{\sigma}} + \mathbf{V}^{\mathrm{t}}\dot{\boldsymbol{\sigma}} = 0 \tag{46}$$

are satisfied, from Eq. (44) it follows that

$$q_y^2\dot{\lambda} = \boldsymbol{\sigma}^{\mathrm{t}}\dot{\boldsymbol{\varepsilon}} + \mathbf{V}^{\mathrm{t}}\mathbf{K}\dot{\boldsymbol{\varepsilon}}, \tag{47}$$

where

$$q_y := \sqrt{2S_y + \mathbf{V}^{\mathrm{t}}\mathbf{K}\mathbf{V}}. \tag{48}$$

Thus, the straining condition $\boldsymbol{\sigma}^{\mathrm{t}}\dot{\boldsymbol{\varepsilon}} + \mathbf{V}^{\mathrm{t}}\mathbf{K}\dot{\boldsymbol{\varepsilon}} > 0$ and the yield condition $\boldsymbol{\sigma}^{\mathrm{t}}\mathbf{K}^{-1}\boldsymbol{\sigma} + 2\mathbf{V}^{\mathrm{t}}\boldsymbol{\sigma} = 2S_y$ are sufficient and necessary for the plastic irreversibility $\dot{\lambda} > 0$. Considering Eq. (47) together with Eqs. (37) and (38), we obtain the following on–off switching criteria for the mechanism of plasticity:

$$\dot{\lambda} = \frac{\boldsymbol{\sigma}^{\mathrm{t}}\dot{\boldsymbol{\varepsilon}} + \mathbf{V}^{\mathrm{t}}\mathbf{K}\dot{\boldsymbol{\varepsilon}}}{q_y^2} > 0 \quad \text{if } \boldsymbol{\sigma}^{\mathrm{t}}\mathbf{K}^{-1}\boldsymbol{\sigma} + 2\mathbf{V}^{\mathrm{t}}\boldsymbol{\sigma} = 2S_y \text{ and } \boldsymbol{\sigma}^{\mathrm{t}}\dot{\boldsymbol{\varepsilon}} + \mathbf{V}^{\mathrm{t}}\mathbf{K}\dot{\boldsymbol{\varepsilon}} > 0, \tag{49}$$

$$\dot{\lambda} = 0 \quad \text{if } \boldsymbol{\sigma}^{\mathrm{t}}\mathbf{K}^{-1}\boldsymbol{\sigma} + 2\mathbf{V}^{\mathrm{t}}\boldsymbol{\sigma} < 2S_y \text{ or } \boldsymbol{\sigma}^{\mathrm{t}}\dot{\boldsymbol{\varepsilon}} + \mathbf{V}^{\mathrm{t}}\mathbf{K}\dot{\boldsymbol{\varepsilon}} \leqslant 0. \tag{50}$$

Substituting the above $\dot{\lambda}$ into Eq. (41) we obtain the two-phase governing equations:

$$\dot{\boldsymbol{\sigma}} = \mathbf{K}\dot{\boldsymbol{\varepsilon}} - \frac{(\boldsymbol{\sigma} + \mathbf{KV})^{\mathrm{t}}\dot{\boldsymbol{\varepsilon}}}{q_y^2}(\boldsymbol{\sigma} + \mathbf{KV}) \quad \text{if } \boldsymbol{\sigma}^{\mathrm{t}}\mathbf{K}^{-1}\boldsymbol{\sigma} + 2\mathbf{V}^{\mathrm{t}}\boldsymbol{\sigma} = 2S_y \text{ and } \boldsymbol{\sigma}^{\mathrm{t}}\dot{\boldsymbol{\varepsilon}} + \mathbf{V}^{\mathrm{t}}\mathbf{K}\dot{\boldsymbol{\varepsilon}} > 0, \tag{51}$$

$$\dot{\boldsymbol{\sigma}} = \mathbf{K}\dot{\boldsymbol{\varepsilon}} \quad \text{if } \boldsymbol{\sigma}^{\mathrm{t}}\mathbf{K}^{-1}\boldsymbol{\sigma} + 2\mathbf{V}^{\mathrm{t}}\boldsymbol{\sigma} < 2S_y \text{ or } \boldsymbol{\sigma}^{\mathrm{t}}\dot{\boldsymbol{\varepsilon}} + \mathbf{V}^{\mathrm{t}}\mathbf{K}\dot{\boldsymbol{\varepsilon}} \leqslant 0. \tag{52}$$

As can be seen the elastic equation is easy to solve; however, the plastic equation is more complex for appearing a quadratic term in Eq. (51). In the following we are going to reduce the non-linear plastic equation to a linear one through a group-theoretic approach.

## 5. Non-canonical Minkowski spacetime formulation

Let us define the integrating factor

$$\mathscr{X}_0 := \exp\lambda, \tag{53}$$

and taking the product of it with Eq. (41) yields

$$\mathbf{K}^{-1}\mathscr{X}_0\dot{\boldsymbol{\sigma}} + (\mathbf{K}^{-1}\boldsymbol{\sigma} + \mathbf{V})\dot{\mathscr{X}}_0 = \mathscr{X}_0\dot{\boldsymbol{\varepsilon}}, \tag{54}$$

where

$$\dot{\mathscr{X}}_0 = \mathscr{X}_0\dot{\lambda} = \mathscr{X}_0\frac{\boldsymbol{\sigma}^{\mathrm{t}}\dot{\boldsymbol{\varepsilon}} + \mathbf{V}^{\mathrm{t}}\mathbf{K}\dot{\boldsymbol{\varepsilon}}}{q_y^2} \tag{55}$$

obtained from Eqs. (49) and (53), was used.

Let us define

$$\boldsymbol{\mathscr{X}} = \begin{bmatrix} \boldsymbol{\mathscr{X}}_s \\ \mathscr{X}_0 \end{bmatrix} := \begin{bmatrix} \mathscr{X}_0\boldsymbol{\sigma} \\ \mathscr{X}_0 \end{bmatrix}, \tag{56}$$

and call it the $n+1$-dimensional augmented stress vector. Note that the components of the stress vector $\boldsymbol{\sigma}$ and the components of the augmented stress vector $\boldsymbol{\mathscr{X}}$ are indeed the non-homogeneous and homogeneous coordinates of the same stress state. Two augmented stress vectors which only differ by a non-zero scalar multiple represent the same stress vector.

Consider the following non-canonical Minkowski metric tensor:

$$\boldsymbol{\mathscr{G}} := \begin{bmatrix} \mathbf{K}^{-1} & \mathbf{V} \\ \mathbf{V}^{\mathrm{t}} & -2S_y \end{bmatrix}, \tag{57}$$

and then by Eq. (56) we have

$$\boldsymbol{\mathscr{X}}^{\mathrm{t}}\boldsymbol{\mathscr{G}}\boldsymbol{\mathscr{X}} = \mathscr{X}_0^2[\boldsymbol{\sigma}^{\mathrm{t}}\mathbf{K}^{-1}\boldsymbol{\sigma} + 2\mathbf{V}^{\mathrm{t}}\boldsymbol{\sigma} - 2S_y]. \tag{58}$$

Reminding $\mathscr{X}_0 > 0$ in Eq. (53), we may further distinguish two correspondences:

$$\boldsymbol{\sigma}^{\mathrm{t}}\mathbf{K}^{-1}\boldsymbol{\sigma} + 2\mathbf{V}^{\mathrm{t}}\boldsymbol{\sigma} = 2S_y \Longleftrightarrow \boldsymbol{\mathscr{X}}^{\mathrm{t}}\boldsymbol{\mathscr{G}}\boldsymbol{\mathscr{X}} = 0, \tag{59}$$

$$\boldsymbol{\sigma}^{\mathrm{t}}\mathbf{K}^{-1}\boldsymbol{\sigma} + 2\mathbf{V}^{\mathrm{t}}\boldsymbol{\sigma} < 2S_y \Longleftrightarrow \boldsymbol{\mathscr{X}}^{\mathrm{t}}\boldsymbol{\mathscr{G}}\boldsymbol{\mathscr{X}} < 0. \tag{60}$$

According to the above results, we can recast the model postulated in Eqs. (34)–(39) to a model in the augmented stress space of $\boldsymbol{\mathscr{X}}$ (see Appendix A):

$$\begin{bmatrix} \mathbf{K}^{-1} & \mathbf{V} \\ \mathbf{V}^{\mathrm{t}} & -2S_y \end{bmatrix} \frac{\mathrm{d}}{\mathrm{d}t} \begin{bmatrix} \mathscr{X}_0\boldsymbol{\sigma} \\ \mathscr{X}_0 \end{bmatrix} = \begin{bmatrix} \mathbf{0} & \dot{\boldsymbol{\varepsilon}} \\ -\dot{\boldsymbol{\varepsilon}}^{\mathrm{t}} & 0 \end{bmatrix} \begin{bmatrix} \mathscr{X}_0\boldsymbol{\sigma} \\ \mathscr{X}_0 \end{bmatrix} \quad \text{if } \boldsymbol{\mathscr{X}}^{\mathrm{t}}\boldsymbol{\mathscr{G}}\boldsymbol{\mathscr{X}} = 0 \text{ and } \dot{\mathscr{X}}_0 > 0. \tag{61}$$

Correspondingly, in the elastic phase we have

$$\begin{bmatrix} \mathbf{K}^{-1} & \mathbf{V} \\ \mathbf{V}^{\mathrm{t}} & -2S_y \end{bmatrix} \frac{\mathrm{d}}{\mathrm{d}t} \begin{bmatrix} \mathscr{X}_0\boldsymbol{\sigma} \\ \mathscr{X}_0 \end{bmatrix} = \begin{bmatrix} \mathbf{0} & \dot{\boldsymbol{\varepsilon}} \\ \mathbf{0} & \mathbf{V}^{\mathrm{t}}\mathbf{K}\dot{\boldsymbol{\varepsilon}} \end{bmatrix} \begin{bmatrix} \mathscr{X}_0\boldsymbol{\sigma} \\ \mathscr{X}_0 \end{bmatrix} \quad \text{if } \boldsymbol{\mathscr{X}}^{\mathrm{t}}\boldsymbol{\mathscr{G}}\boldsymbol{\mathscr{X}} < 0 \text{ or } \dot{\mathscr{X}}_0 = 0. \tag{62}$$

That the conditions of the above two equations hold are due to

$$\boldsymbol{\mathscr{X}}^{\mathrm{t}}\boldsymbol{\mathscr{G}}\boldsymbol{\mathscr{X}} \leqslant 0, \tag{63}$$

$$\dot{\mathscr{X}}_0 \geqslant 0, \tag{64}$$

which correspond to the inequalities (37) and (38), respectively.

Multiplying Eq. (62) by

$$\begin{bmatrix} \mathbf{K}^{-1} & \mathbf{V} \\ \mathbf{V}^{\mathrm{t}} & -2S_y \end{bmatrix}^{-1} = \begin{bmatrix} \mathbf{K} - \frac{1}{q_y^2}\mathbf{K}\mathbf{V}\mathbf{V}^{\mathrm{t}}\mathbf{K} & \frac{1}{2S_y}(\mathbf{K} - \frac{1}{q_y^2}\mathbf{K}\mathbf{V}\mathbf{V}^{\mathrm{t}}\mathbf{K})\mathbf{V} \\ \frac{1}{2S_y}\mathbf{V}^{\mathrm{t}}(\mathbf{K} - \frac{1}{q_y^2}\mathbf{K}\mathbf{V}\mathbf{V}^{\mathrm{t}}\mathbf{K}) & -\frac{1}{q_y^2} \end{bmatrix} \tag{65}$$

we get

$$\frac{\mathrm{d}}{\mathrm{d}t} \begin{bmatrix} \mathscr{X}_0\boldsymbol{\sigma} \\ \mathscr{X}_0 \end{bmatrix} = \begin{bmatrix} \mathbf{0} & \mathbf{K}\dot{\boldsymbol{\varepsilon}} \\ \mathbf{0} & 0 \end{bmatrix} \begin{bmatrix} \mathscr{X}_0\boldsymbol{\sigma} \\ \mathscr{X}_0 \end{bmatrix}. \tag{66}$$

Since the last row leads to $\dot{\mathscr{X}}_0 = 0$, which means that $\mathscr{X}_0$ is a constant, the elastic equation $\dot{\boldsymbol{\sigma}} = \mathbf{K}\dot{\boldsymbol{\varepsilon}}$ is recovered after eliminating the $\mathscr{X}_0$ in $\mathrm{d}(\mathscr{X}_0\boldsymbol{\sigma})/\mathrm{d}t = \mathscr{X}_0\mathbf{K}\dot{\boldsymbol{\varepsilon}}$ obtained from the first row. On the other hand, rearranging Eq. (61) with the help of Eq. (65) we get

$$\dot{\boldsymbol{\mathscr{X}}} = \mathbf{B}\boldsymbol{\mathscr{X}}, \tag{67}$$

where

$$\mathbf{B} := \begin{bmatrix} \frac{1}{2S_y}\left(\frac{1}{q_y^2}\mathbf{K}\mathbf{V}\mathbf{V}^{\mathrm{t}}\mathbf{K} - \mathbf{K}\right)\mathbf{V}\dot{\boldsymbol{\varepsilon}}^{\mathrm{t}} & \left(\mathbf{K} - \frac{1}{q_y^2}\mathbf{K}\mathbf{V}\mathbf{V}^{\mathrm{t}}\mathbf{K}\right)\dot{\boldsymbol{\varepsilon}} \\ \frac{1}{q_y^2}\dot{\boldsymbol{\varepsilon}}^{\mathrm{t}} & \frac{1}{2S_y}\mathbf{V}^{\mathrm{t}}\left(\mathbf{K} - \frac{1}{q_y^2}\mathbf{K}\mathbf{V}\mathbf{V}^{\mathrm{t}}\mathbf{K}\right)\dot{\boldsymbol{\varepsilon}} \end{bmatrix}. \tag{68}$$

When compared with the plastic equation (51) it is obvious that the above plastic equation is linear and is more easy to integrate. Even not so clear, the above state matrix $\mathbf{B}$ is indeed an element of the Lie algebra of the special orthochronous pseudo-linear group $\mathrm{SL}(n, 1, \mathbb{R})$, since the trace of $\mathbf{B}$ is zero. However, it can be reduced to a more simple form below.

## 6. Reduction to a canonical form

The metric tensor $\mathscr{G}$ in Eq. (58) is not a canonical one; however, if we use

$$\mathbf{P} = \begin{bmatrix} \mathbf{K}^{1/2} & \mathbf{0}_{n\times 1} \\ -q_y^{-1}\mathbf{V}^{\mathrm{t}}\mathbf{K} & q_y^{-1} \end{bmatrix}, \tag{69}$$

it is easy to check that the following transformation holds:

$$\mathbf{P}\mathscr{G}\mathbf{P}^{\mathrm{t}} = \mathbf{g}, \tag{70}$$

where

$$\mathbf{g} := \begin{bmatrix} \mathbf{I}_n & \mathbf{0}_{n\times 1} \\ \mathbf{0}_{1\times n} & -1 \end{bmatrix} \tag{71}$$

is a canonical Minkowski metric tensor.

With the aid of the above transformation matrix given in Eq. (69) we can introduce a canonical augmented stress vector

$$\mathbf{X} := \mathbf{P}^{-t}\mathscr{X} = \begin{bmatrix} \mathbf{K}^{-1/2} & \mathbf{K}^{1/2}\mathbf{V} \\ \mathbf{0}_{1\times n} & q_y \end{bmatrix} \mathscr{X} \tag{72}$$

as a new variable. So we can obtain

$$\mathscr{X}^{\mathrm{t}}\mathscr{G}\mathscr{X} = \mathbf{X}^{\mathrm{t}}\mathbf{g}\mathbf{X} \tag{73}$$

due to Eq. (70), and simultaneously Eq. (61) reduces to

$$\dot{\mathbf{X}} = \mathbf{A}\mathbf{X}, \tag{74}$$

where

$$\mathbf{A} := \frac{1}{q_y}\begin{bmatrix} \mathbf{0}_n & \mathbf{K}^{1/2}\dot{\boldsymbol{\varepsilon}} \\ \dot{\boldsymbol{\varepsilon}}^{\mathrm{t}}\mathbf{K}^{1/2} & 0 \end{bmatrix}. \tag{75}$$

It is obvious that

$$\mathbf{A}^{\mathrm{t}}\mathbf{g} + \mathbf{g}\mathbf{A} = \mathbf{0}. \tag{76}$$

By Eq. (74) the solution is more easy to derive than Eq. (67). Denote the fundamental solution by $\mathbf{G}(t)$, i.e.,

$$\dot{\mathbf{G}}(t) = \mathbf{A}(t)\mathbf{G}(t), \qquad \mathbf{G}(0) = \mathbf{I}_{n+1}. \tag{77}$$

From Liu (2001b) it is known that $\mathbf{G}(t)$ is an element of the proper orthochronous Lorentz group $\mathrm{SO_o}(n,1)$, since $\mathbf{A}(t)$ is a Lie algebra of $\mathrm{so}(n,1)$, satisfying

$$\mathbf{G}^{\mathrm{t}}(t)\mathbf{g}\mathbf{G}(t) = \mathbf{g}, \tag{78}$$

$$\det \mathbf{G} = 1, \tag{79}$$

$$G_0^0 \geqslant 1. \tag{80}$$

Thus, the solution of Eq. (74) can be expressed as

$$\mathbf{X}(t) = [\mathbf{G}(t)\mathbf{G}^{-1}(t_1)]\mathbf{X}(t_1) \quad \forall t, t_1 \in I_{\mathrm{on}}, \tag{81}$$

where $I_{\text{on}}$ denotes a time interval within which plasticity is working. To elaborate, we solve Eq. (78) for the inverse

$$\mathbf{G}^{-1} = \mathbf{g}\mathbf{G}^{\mathrm{t}}\mathbf{g}, \tag{82}$$

and partition $\mathbf{G}$ as

$$\mathbf{G} = \begin{bmatrix} \mathbf{G}_s^s & \mathbf{G}_0^s \\ \mathbf{G}_s^0 & G_0^0 \end{bmatrix}. \tag{83}$$

Thus, the solution of $\mathbf{X}(t)$ is

$$\mathbf{X}(t) = \begin{bmatrix} \mathbf{G}_s^s(t)(\mathbf{G}_s^s)^{\mathrm{t}}(t_1) - \mathbf{G}_0^s(t)(\mathbf{G}_0^s)^{\mathrm{t}}(t_1) & \mathbf{G}_0^s(t)G_0^0(t_1) - \mathbf{G}_s^s(t)\mathbf{G}_s^0(t_1) \\ \mathbf{G}_s^0(t)(\mathbf{G}_s^s)^{\mathrm{t}}(t_1) - G_0^0(t)(\mathbf{G}_0^s)^{\mathrm{t}}(t_1) & G_0^0(t)G_0^0(t_1) - \mathbf{G}_s^0(t)\mathbf{G}_s^0(t_1) \end{bmatrix} \mathbf{X}(t_1). \tag{84}$$

By Eqs. (72) and (84) the solution of $\mathscr{X}$ is found to be

$$\mathscr{X}(t) = \begin{bmatrix} \mathbf{K}^{1/2} & -q_y^{-1}\mathbf{K}\mathbf{V} \\ \mathbf{0}_{1\times n} & q_y^{-1} \end{bmatrix} \begin{bmatrix} \mathbf{G}_s^s(t)(\mathbf{G}_s^s)^{\mathrm{t}}(t_1) - \mathbf{G}_0^s(t)(\mathbf{G}_0^s)^{\mathrm{t}}(t_1) & \mathbf{G}_0^s(t)G_0^0(t_1) - \mathbf{G}_s^s(t)\mathbf{G}_s^0(t_1) \\ \mathbf{G}_s^0(t)(\mathbf{G}_s^s)^{\mathrm{t}}(t_1) - G_0^0(t)(\mathbf{G}_0^s)^{\mathrm{t}}(t_1) & G_0^0(t)G_0^0(t_1) - \mathbf{G}_s^0(t)\mathbf{G}_s^0(t_1) \end{bmatrix} \begin{bmatrix} \mathbf{K}^{-1/2} & \mathbf{K}^{1/2}\mathbf{V} \\ \mathbf{0}_{1\times n} & q_y \end{bmatrix} \mathscr{X}(t_1). \tag{85}$$

Then, dividing the first row by the second row of the above solution we obtain $\boldsymbol{\sigma}$ in view of Eq. (56). The other approach to the canonical form in Eq. (74) is given in Appendix B.

## 7. Numerical methods for the strain-energy yielding model

### 7.1. Cubic symmetry material

In the model simulation we only consider a cubic symmetry material for simplicity. For symmetry of the cubic system, the determination of the reference coordinate system should correspond to the cubic system axes [1 0 0], [0 1 0] and [0 0 1]. And, the stiffness tensor can be simplified in the easiest form:

$$\mathbf{K} = \begin{bmatrix} K_{11} & K_{12} & K_{12} & 0 & 0 & 0 \\ & K_{11} & K_{12} & 0 & 0 & 0 \\ & & K_{11} & 0 & 0 & 0 \\ & & & K_{44} & 0 & 0 \\ & \text{Sym.} & & & K_{44} & 0 \\ & & & & & K_{44} \end{bmatrix}. \tag{86}$$

For the cubic materials there have only three independent elastic constants in $\mathbf{K}$. The other three constant matrices needed in the above calculations are given as follows:

$$\mathbf{K}^{1/2} = \begin{bmatrix} F_1 & F_2 & F_2 & 0 & 0 & 0 \\ & F_1 & F_2 & 0 & 0 & 0 \\ & & F_1 & 0 & 0 & 0 \\ & & & \sqrt{K_{44}} & 0 & 0 \\ & \text{Sym.} & & & \sqrt{K_{44}} & 0 \\ & & & & & \sqrt{K_{44}} \end{bmatrix}, \tag{87}$$

$$\mathbf{K}^{-1/2}=\begin{bmatrix} F_3 & F_4 & F_4 & 0 & 0 & 0 \\ & F_3 & F_4 & 0 & 0 & 0 \\ & & F_3 & 0 & 0 & 0 \\ & & & \frac{1}{\sqrt{K_{44}}} & 0 & 0 \\ & \text{Sym.} & & & \frac{1}{\sqrt{K_{44}}} & 0 \\ & & & & & \frac{1}{\sqrt{K_{44}}} \end{bmatrix}, \tag{88}$$

$$\mathbf{K}^{-1}=\begin{bmatrix} F_5 & F_6 & F_6 & 0 & 0 & 0 \\ & F_5 & F_6 & 0 & 0 & 0 \\ & & F_5 & 0 & 0 & 0 \\ & & & \frac{1}{K_{44}} & 0 & 0 \\ & \text{Sym.} & & & \frac{1}{K_{44}} & 0 \\ & & & & & \frac{1}{K_{44}} \end{bmatrix}, \tag{89}$$

where

$$F_1:=\frac{2\sqrt{K_{11}-K_{12}}}{3}+\frac{\sqrt{K_{11}+2K_{12}}}{3},\qquad F_2:=\frac{-\sqrt{K_{11}-K_{12}}}{3}+\frac{\sqrt{K_{11}+2K_{12}}}{3},$$

$$F_3:=\frac{2}{3\sqrt{K_{11}-K_{12}}}+\frac{1}{3\sqrt{K_{11}+2K_{12}}},\qquad F_4:=\frac{-1}{3\sqrt{K_{11}-K_{12}}}+\frac{1}{3\sqrt{K_{11}+2K_{12}}},$$

$$F_5:=\frac{2}{3(K_{11}-K_{12})}+\frac{1}{3(K_{11}+2K_{12})},\qquad F_6:=\frac{-1}{3(K_{11}-K_{12})}+\frac{1}{3(K_{11}+2K_{12})}.$$

### 7.2. Strain control

Consider a rectilinear strain path with a non-zero constant strain rate,

$$\dot{\boldsymbol{\varepsilon}}=\text{constant}\neq\mathbf{0}, \tag{90}$$

and starting from $\boldsymbol{\varepsilon}(t_1)$ at time $t_1$. The constitutive response can be determined exactly, and it may be recast to the form of Eq. (81) with the canonically augmented stress transition group in the on phase being

$$\mathbf{G}(t)\mathbf{G}^{-1}(t_1)=\begin{bmatrix} \mathbf{I}_n+\mathbf{M}_1 & \frac{b\mathbf{V}_1}{\|\mathbf{V}_1\|} \\ \frac{b\mathbf{V}_1^{\mathrm{t}}}{\|\mathbf{V}_1\|} & a \end{bmatrix}, \tag{91}$$

where

$$\mathbf{V}_1:=\mathbf{K}^{1/2}\dot{\boldsymbol{\varepsilon}},\quad \mathbf{M}_1:=\frac{(a-1)}{\|\mathbf{V}_1\|^2}\mathbf{V}_1\mathbf{V}_1^{\mathrm{t}}, \tag{92}$$

$$a:=\cosh[(t-t_1)\|\mathbf{V}_1\|/q_y],\quad b:=\sinh[(t-t_1)\|\mathbf{V}_1\|/q_y], \tag{93}$$

and $\|\mathbf{V}_1\|$ denotes the Euclidean norm of $\mathbf{V}_1$.

Substituting Eq. (81) into Eq. (72) gives

$$\mathscr{X}(t)=\mathbf{P}^{\mathrm{t}}\mathbf{G}(t)\mathbf{G}^{-1}(t_1)\mathbf{P}^{-t}\mathscr{X}(t_1)\quad\forall t,t_1\in I_{\mathrm{on}}. \tag{94}$$

From Eqs. (56) and (91) we get

$$\begin{bmatrix} \mathscr{X}_0(t)\boldsymbol{\sigma}(t) \\ \mathscr{X}_0(t) \end{bmatrix} = \begin{bmatrix} \mathbf{I}_n + \mathbf{K}^{1/2}\mathbf{M}_1\mathbf{K}^{-1/2} - \mathbf{M}_2\mathbf{K}^{-1/2} & (1-a)\mathbf{K}\mathbf{V} + \mathbf{V}_2 \\ \frac{b}{q_y\|\mathbf{V}_1\|}\mathbf{V}_1^{\mathrm{t}}\mathbf{K}^{-1/2} & a + \frac{b}{q_y\|\mathbf{V}_1\|}\mathbf{V}_1^{\mathrm{t}}\mathbf{K}^{1/2}\mathbf{V} \end{bmatrix} \begin{bmatrix} \mathscr{X}_0(t_1)\boldsymbol{\sigma}(t_1) \\ \mathscr{X}_0(t_1) \end{bmatrix}, \tag{95}$$

where

$$\mathbf{M}_2 := \frac{b\mathbf{K}\mathbf{V}\mathbf{V}_1^{\mathrm{t}}}{q_y\|\mathbf{V}_1\|}, \tag{96}$$

$$\mathbf{V}_2 := \frac{bq_y\mathbf{K}^{1/2}\mathbf{V}_1}{\|\mathbf{V}_1\|} + \mathbf{K}^{1/2}\mathbf{M}_1\mathbf{K}^{1/2}\mathbf{V} - \mathbf{M}_2\mathbf{K}^{1/2}\mathbf{V}. \tag{97}$$

Dividing the first row by the second row in Eq. (95) we obtain

$$\frac{\boldsymbol{\sigma}(t)}{q_y\|\mathbf{V}_1\|} = \frac{[\mathbf{I}_n + \mathbf{K}^{1/2}\mathbf{M}_1\mathbf{K}^{-1/2} - \mathbf{M}_2\mathbf{K}^{-1/2}]\boldsymbol{\sigma}(t_1) + (1-a)\mathbf{K}\mathbf{V} + \mathbf{V}_2}{aq_y\|\mathbf{V}_1\| + b\mathbf{V}_1^{\mathrm{t}}\mathbf{K}^{-1/2}\boldsymbol{\sigma}(t_1) + b\mathbf{V}_1^{\mathrm{t}}\mathbf{K}^{1/2}\mathbf{V}}. \tag{98}$$

This is the stress response in the on phase, while in the off phase it is replaced by

$$\boldsymbol{\sigma}(t) = \boldsymbol{\sigma}(t_1) + \mathbf{K}[\boldsymbol{\varepsilon}(t) - \boldsymbol{\varepsilon}(t_1)]. \tag{99}$$

Substituting Eq. (99) into the yield condition (29) we obtain a quadratic equation for $t - t_1$:

$$A(t-t_1)^2 + B(t-t_1) + C = 0, \tag{100}$$

where

$$A = \dot{\boldsymbol{\varepsilon}}^{\mathrm{t}}\mathbf{K}\dot{\boldsymbol{\varepsilon}},$$

$$B := 2\dot{\boldsymbol{\varepsilon}}^{\mathrm{t}}\boldsymbol{\sigma}(t_1) + 2\dot{\boldsymbol{\varepsilon}}^{\mathrm{t}}\mathbf{K}\mathbf{V},$$

$$C := \boldsymbol{\sigma}^{\mathrm{t}}(t_1)\mathbf{K}^{-1}\boldsymbol{\sigma}(t_1) + 2\mathbf{V}^{\mathrm{t}}\boldsymbol{\sigma}(t_1) - 2S_y.$$

Thus, we have

$$t_{\mathrm{on}} = \begin{cases} t_1 & \text{if } C = 0 \text{ and } B \geqslant 0, \\ t_1 - \frac{B}{A} & \text{if } C = 0 \text{ and } B < 0, \\ t_1 + \frac{\sqrt{B^2 - 4AC} - B}{2A} & \text{if } C < 0. \end{cases} \tag{101}$$

Now, let us apply the above solutions to a certain example. The material constants used in the calculation were $K_{11} = 463\,000$ MPa, $K_{12} = 161\,000$ MPa, $K_{44} = 109\,000$ MPa, and $S_y = 0.25$ MPa. Fig. 1 displays a rectangular strain path, the corresponding stress path and the stress–strain curves in the axial and torsional directions under the strain inputs within two cycles.

For arbitrary specified strain path the above calculation method is also good to preserve the consistent condition, since we can approximate the specified controlled-strain path by many rectilinear strain paths, such that $\dot{\boldsymbol{\varepsilon}}$ at each time step is a constant vector, and then we can calculate the next step response of $\boldsymbol{\sigma}(t)$ by Eq. (98) with a known $\boldsymbol{\sigma}(t_1)$ at the previous time step.

### 7.3. Stress control

Eq. (51) can be rewritten as

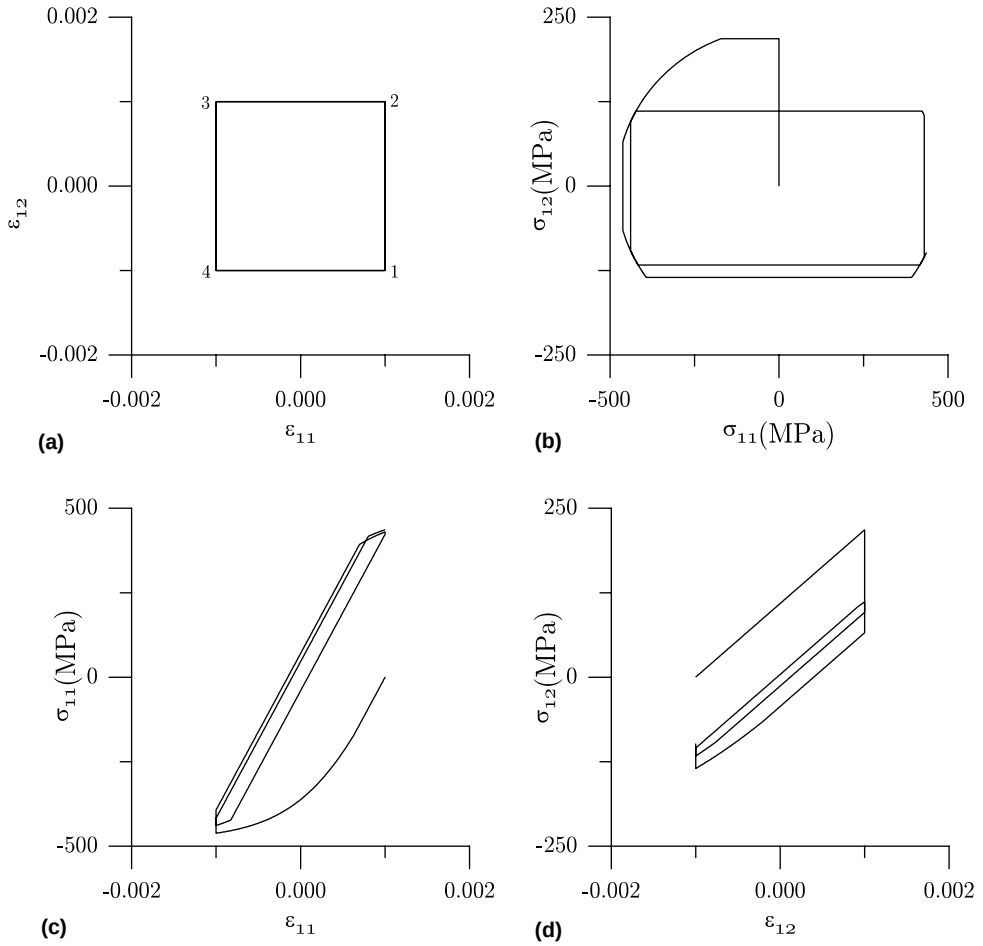


Fig. 1. The responses of strain-energy yielding model to an input of cyclic square strain path in (a), and (b) displaying its corresponding stress path, (c) the cyclic axial stress–axial strain curve, and (d) the cyclic shear stress–shear strain curve.

$$\mathbf{K}^{-1}\dot{\boldsymbol{\sigma}} = \left[\mathbf{I}_n - \frac{1}{q_y^2}(\mathbf{K}^{-1}\boldsymbol{\sigma} + \mathbf{V}) \otimes (\boldsymbol{\sigma} + \mathbf{K}\mathbf{V})\right]\dot{\boldsymbol{\varepsilon}}, \tag{102}$$

where $\otimes$ denotes the dyadic product, and $q_y$ was defined by Eq. (48).

In the plastic phase the stress control is not permitted; however, we consider the smoothing factor technique introduced by Liu (2003b) into the new model, which allows plasticity to happen inside the yield surface, such that from Eq. (102) we have

$$\begin{aligned}\dot{\boldsymbol{\varepsilon}} &= \left[\mathbf{I}_n - \frac{1}{q_y^2}(\mathbf{K}^{-1}\boldsymbol{\sigma} + \mathbf{V}) \otimes (\boldsymbol{\sigma} + \mathbf{K}\mathbf{V})\right]^{-1} \mathbf{K}^{-1}\dot{\boldsymbol{\sigma}} = \mathbf{K}^{-1}\dot{\boldsymbol{\sigma}} + \frac{\boldsymbol{\sigma}^{\mathrm{t}}\mathbf{K}^{-1}\dot{\boldsymbol{\sigma}} + \mathbf{V}^{\mathrm{t}}\dot{\boldsymbol{\sigma}}}{2S_y - \boldsymbol{\sigma}^{\mathrm{t}}\mathbf{K}^{-1}\boldsymbol{\sigma} - 2\mathbf{V}^{\mathrm{t}}\boldsymbol{\sigma}}[\mathbf{K}^{-1}\boldsymbol{\sigma} + \mathbf{V}] \\ &= \mathbf{K}^{-1}\dot{\boldsymbol{\sigma}} + \dot{\lambda}[\mathbf{K}^{-1}\boldsymbol{\sigma} + \mathbf{V}].\end{aligned} \tag{103}$$

From Eqs. (34)–(36) the above last equality follows. The above equation is well defined by controlling the stress in the range of $2S_y - \boldsymbol{\sigma}^{\mathrm{t}}\mathbf{K}^{-1}\boldsymbol{\sigma} - 2\mathbf{V}^{\mathrm{t}}\boldsymbol{\sigma} > 0$.

By inserting Eq. (41) for $\dot{\boldsymbol{\varepsilon}}$ into Eq. (47), and then using Eqs. (40) and (48) we obtain

$$\dot{\lambda} f(\boldsymbol{\sigma}) = -\tfrac{1}{2}\dot{f}(\boldsymbol{\sigma}). \tag{104}$$

Under the stress control in the range of $f < 0$ and the plastic loading condition with $\dot{f} > 0$ from the above equation it is obvious that $\dot{\lambda} > 0$ in the plastic phase. On the other hand, during the elastic phase the strain is calculated by

$$\boldsymbol{\varepsilon}(t) = \boldsymbol{\varepsilon}(t_1) + \mathbf{K}^{-1}[\boldsymbol{\sigma}(t) - \boldsymbol{\sigma}(t_1)], \tag{105}$$

which is obtained by letting $\dot{\lambda} = 0$ in Eq. (103) and integrating the resultant from $t_1$ to $t$. Therefore, as the original model is, the new model modified by a smoothing factor is thermodynamically consistent since $\dot{\lambda} > 0$ in the plastic phase and $\dot{\lambda} = 0$ in the elastic phase.

We consider a rectilinear stress path

$$\boldsymbol{\sigma}(t) = \boldsymbol{\sigma}(t_1) + (t - t_1)\dot{\boldsymbol{\sigma}} \tag{106}$$

starting from an admissible stress point $\boldsymbol{\sigma}(t_1)$ at time $t_1$ with

$$\dot{\boldsymbol{\sigma}} = \text{constant} \neq \mathbf{0}. \tag{107}$$

Substituting Eq. (106) into the yield condition (29) we obtain a quadratic equation for $t - t_1$:

$$A(t - t_1)^2 + B(t - t_1) + C = 0, \tag{108}$$

where

$$A = \dot{\boldsymbol{\sigma}}^{\mathrm{t}}\mathbf{K}^{-1}\dot{\boldsymbol{\sigma}},$$

$$B := 2\dot{\boldsymbol{\sigma}}^{\mathrm{t}}\mathbf{K}^{-1}\boldsymbol{\sigma}(t_1) + 2\mathbf{V}^{\mathrm{t}}\dot{\boldsymbol{\sigma}},$$

$$C := \boldsymbol{\sigma}^{\mathrm{t}}(t_1)\mathbf{K}^{-1}\boldsymbol{\sigma}(t_1) + 2\mathbf{V}^{\mathrm{t}}\boldsymbol{\sigma}(t_1) - 2S_y.$$

Since $\boldsymbol{\sigma}(t_1)$ is an admissible stress, we have $C < 0$. Thus, solving Eq. (108) for $t$ denoted by $t'$ we get

$$t' = t_1 + \frac{\sqrt{B^2 - 4AC} - B}{2A}. \tag{109}$$

In order to be stress controllable we initiate the plastic mechanism at a much shorter time denoted by $t_{\mathrm{on}}$,

$$t_{\mathrm{on}} = t_1 + \frac{t' - t_1}{\rho} = t_1 + \frac{\sqrt{B^2 - 4AC} - B}{2\rho A}, \tag{110}$$

where we call $\rho > 1$ a smoothing factor.

Under the rectilinear stress path (106), Eq. (103) can be integrated to be

$$\boldsymbol{\varepsilon}(t) = \boldsymbol{\varepsilon}(t_1) - r_1(t)[\mathbf{V} + \mathbf{K}^{-1}\boldsymbol{\sigma}(t_1)] + \left[\frac{b}{2c}r_1(t) + \frac{2ac - b^2}{4c}r_2(t)\right]\mathbf{K}^{-1}\dot{\boldsymbol{\sigma}}, \tag{111}$$

where

$$a := 2S_y - 2\mathbf{V}^{\mathrm{t}}\boldsymbol{\sigma}(t_1) - \boldsymbol{\sigma}^{\mathrm{t}}(t_1)\mathbf{K}^{-1}\boldsymbol{\sigma}(t_1), \tag{112}$$

$$b := -2\mathbf{V}^{\mathrm{t}}\dot{\boldsymbol{\sigma}} - 2\boldsymbol{\sigma}^{\mathrm{t}}(t_1)\mathbf{K}^{-1}\dot{\boldsymbol{\sigma}}, \tag{113}$$

$$c = -\dot{\boldsymbol{\sigma}}^{\mathrm{t}}\mathbf{K}^{-1}\dot{\boldsymbol{\sigma}}, \tag{114}$$

$$r_1(t) := \tfrac{1}{2}\ln[a + b(t-t_1) + c(t-t_1)^2] - \tfrac{1}{2}\ln a, \tag{115}$$

$$r_2(t) := \frac{1}{\sqrt{b^2-4ac}}\ln\frac{\left(b+\sqrt{b^2-4ac}\right)\left[b-\sqrt{b^2-4ac}+2c(t-t_1)\right]}{\left(b-\sqrt{b^2-4ac}\right)\left[b+\sqrt{b^2-4ac}+2c(t-t_1)\right]}. \tag{116}$$

### 7.4. Ratcheting behavior

It is experimentally observed that an unsymmetric stress cycle will cause the cyclic creep of strain in the direction of mean stress, also called the strain ratcheting behavior. In Fig. 2 we show some cyclic stress–strain curves for the different initial pre-stresses $\sigma_{12}$ as indicated but with the same $K_{11} = 463\,000$ MPa, $K_{12} = 161\,000$ MPa, $K_{44} = 109\,000$ MPa, $S_y = 0.25$ MPa and $\rho = 2$ for all cases. It shows that the new model is able to reveal the strain ratcheting behavior; furthermore, it is observed that the symmetric stress cycle with a zero mean stress gives no strain ratcheting as shown in Fig. 2(a) and (b), and more large mean-stress leads to more large strain ratcheting as shown in Fig. 2(c)–(h).

The experimental uniaxial/multiaxial ratcheting tests of metals were conducted by many researchers, for example, Jiang and Sehitoglu (1994a,b), Delobelle et al. (1995), McDowell (1995), Mizuno et al. (2000), Kang et al. (2002a,b, 2004), Kang and Gao (2002) and references therein. The major observations for the most metal behavior are the ratcheting rate decreasing cyclically and then the stopping of ratcheting.

The new model modified from a simple strain-energy yielding model was able to simulate the strain ratcheting behavior as shown in Fig. 2; however, the ratcheting was overprediction. How to remedy these defects becomes importance for the new model. For this we turn our attention to the smoothing factor which plays an important role in the modification, and about which we note that the smaller $\rho$ is, the more close to the original model and deviating from the aim of the description of the cyclic plasticity and the ratcheting effect are. On the other hand, the larger $\rho$ is, the more profound of the ratcheting effect is. In order to suppress the ratcheting and relaxation effects, and get a trade-off between these two tendencies we may decrease the value of $\rho$ from a larger value $\rho_2$ to a smaller value $\rho_1$ by letting

$$\rho(\lambda) = \rho_1 + (\rho_2 - \rho_1)\exp(-k\lambda), \quad 1 \leqslant \rho_1 \leqslant \rho_2 \leqslant 2 \tag{117}$$

when the plasticity going on. Rather than the constant $\rho$ used in the above simulations as shown in Fig. 2, we supposed that the smoothing factor $\rho$ is a scalar function of $\lambda$ calculated by

$$\lambda(t) = \lambda(t_{\mathrm{on}}) + \frac{1}{2}\ln\frac{f(\boldsymbol{\sigma}(t_{\mathrm{on}}))}{f(\boldsymbol{\sigma}(t))}, \tag{118}$$

which is a direct integration of Eq. (104) and the stress control (106) is permitted in the range of $f(\boldsymbol{\sigma}) < 0$.

Under the material constants $K_{11} = 463\,000$ MPa, $K_{12} = 161\,000$ MPa, $K_{44} = 109\,000$ MPa, and $S_y = 0.25$ MPa, in Fig. 3(a) the uniaxial ratchetings under a mean stress $\sigma_{12} = 10$ MPa and a stress amplitude 200 MPa are compared for these by fixing $\rho = 2$ (dashed line) and by employing a scalar function for $\rho$ as defined in Eq. (117) with $\rho_1 = 1$, $\rho_2 = 2$ and $k = 0.8$. The latter result is shown by a solid black line, which can be seen that the ratcheting rate decreases cyclically and the ratcheting tends to saturation gradually. The total ratcheting strain is smaller than the former one that used $\rho = 2$. To simulate the biaxial ratcheting, the stress loading condition is a constant axial stress $\sigma_{11} = 10$ MPa combined with an unsymmetrical shear stress cycle of $\sigma_{12}$ with a mean stress 10 MPa and a stress amplitude of 200 MPa. The calculations show that the biaxial ratcheting takes place not only in the torsional direction but also in the axial

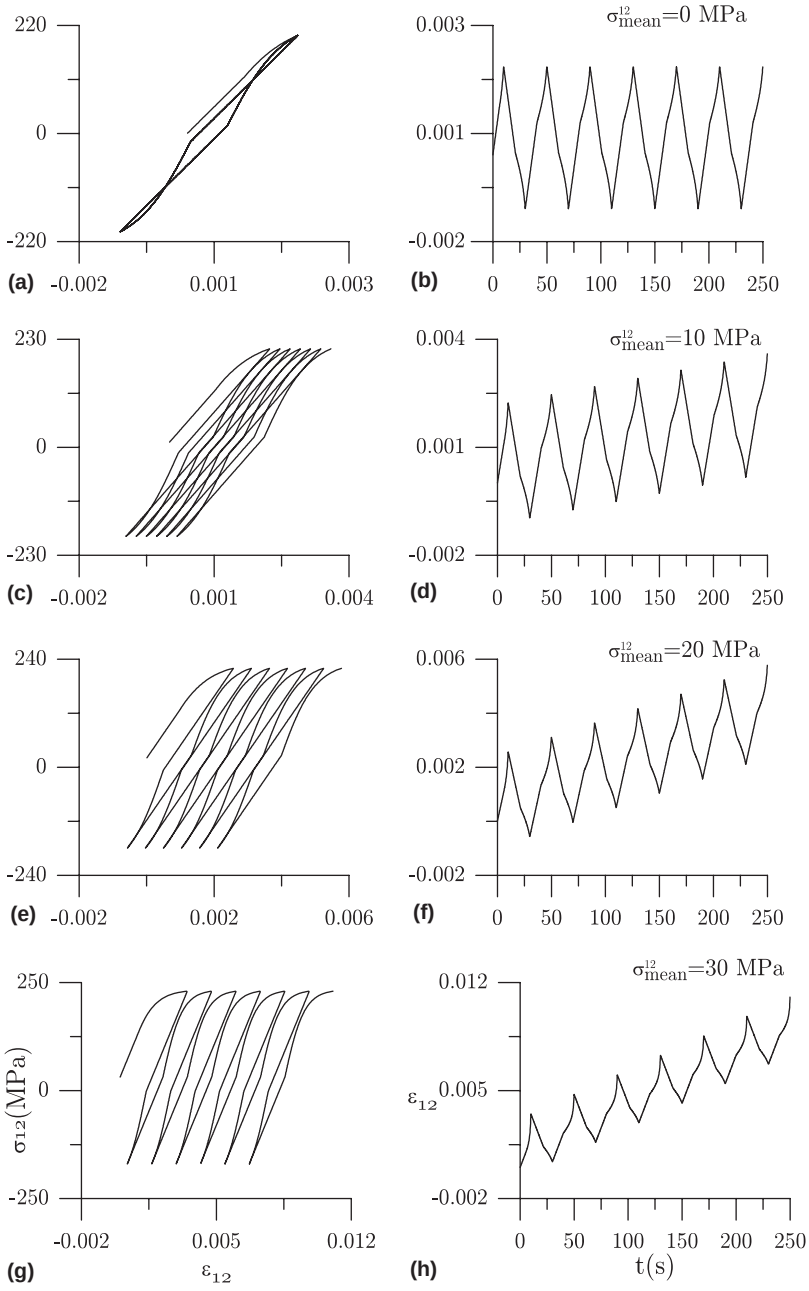


Fig. 2. Under unsymmetric stress cycles the strain ratcheting behavior for the new model is shown for different mean stresses. Larger mean stress renders larger strain ratcheting.

direction due to the non-zero mean shear stress and axial stress. However, the case with a fixing $\rho = 2$ (dashed line) leads to the constant ratcheting rate in two directions and usually over predicts the ratcheting strains. By using the same strategy as above with a variable smoothing factor we obtain a more reasonable biaxial ratcheting behavior as shown by the solid black line in Fig. 3(b).

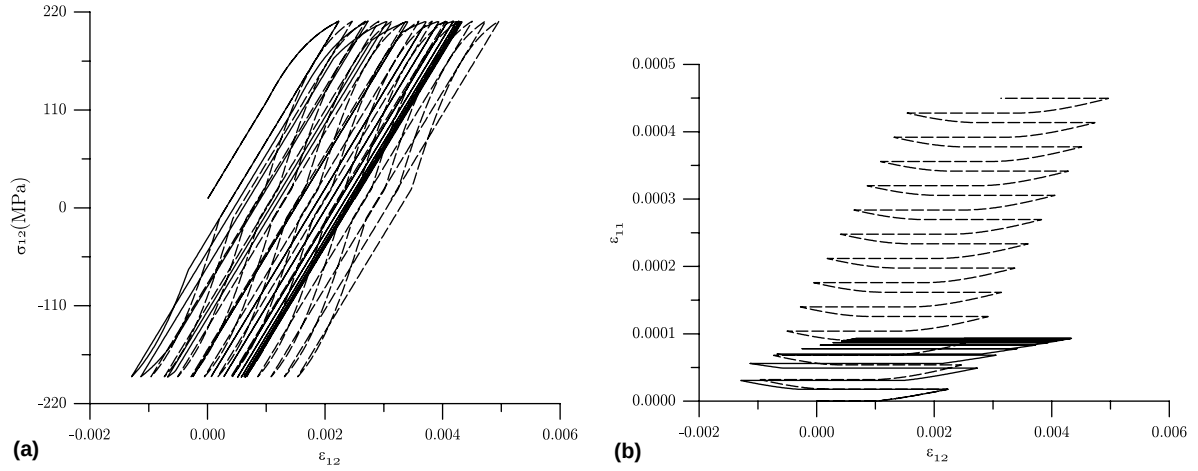


Fig. 3. By employing a scalar function for the smoothing factor in the new model renders a more effective simulation of (a) uniaxial and (b) biaxial ratcheting behaviors under unsymmetric stress loading conditions.

By adjusting the three constants $\rho_1$, $\rho_2$ and $k$ in Eq. (117) we may observe different ratcheting behaviors. Although the replacement of the constant $\rho$ by a scalar function $\rho$ may increase a little computational burden but its effect is increased remarkably. It deserves to note that our model includes no kinematic hardening variables in the formulation. The description of ratcheting by the constitutive equations is usually related to the kinematic hardening mechanism. Several experimental and numerical studies made on metals have shown the inability of the classical kinematic hardening rules to describe the main ratcheting phenomenon. However, a correct simulation of the ratcheting phenomena is still one of the most difficult problems, and there are more accurate and realistic but complex constitutive models that allow to simulate the ratcheting more appropriately, for example, Chaboche (1991, 1994), Voyiadjis and Sivakumar (1991, 1994), Hassan and Kyriakides (1992), Ohno and Wang (1993, 1994), Jiang and Sehitoglu (1994a,b), Delobelle et al. (1995), Corona et al. (1996), Xia and Ellyin (1997), Chaboche and Jung (1998), Taheri and Lorentz (1999), Abdel-Karim and Ohno (2000), Ohno and Abdel-Karim (2000), Portier et al. (2000), Bari and Hassan (2001, 2002). The above lists just reflect an active study of the ratcheting behavior, and the improvements are still in progress.

## 8. Pseudo-Riemann manifold

In this section we consider an anisotropic flow model with a yield criterion (8) and an anisotropic elastic law (9). Here we approach this problem from a different view about the plasticity with a quadratic yield function. Accordingly, we have

$$\dot{\boldsymbol{\sigma}} + \dot{\lambda}\mathbf{K}(\mathbf{C}^{-1}\boldsymbol{\sigma} + \mathbf{V}) = \mathbf{K}\dot{\boldsymbol{\varepsilon}}, \tag{119}$$

where the plastic multiplier $\dot{\lambda}$ is subjecting to the following on–off switching criteria for the mechanism of plasticity:

$$\dot{\lambda} = \frac{(\mathbf{C}^{-1}\boldsymbol{\sigma} + \mathbf{V})^{\mathrm{t}}\mathbf{K}\dot{\boldsymbol{\varepsilon}}}{(\mathbf{C}^{-1}\boldsymbol{\sigma} + \mathbf{V})^{\mathrm{t}}\mathbf{K}(\mathbf{C}^{-1}\boldsymbol{\sigma} + \mathbf{V})} > 0 \quad \text{if } \boldsymbol{\sigma}^{\mathrm{t}}\mathbf{C}^{-1}\boldsymbol{\sigma} + 2\mathbf{V}^{\mathrm{t}}\boldsymbol{\sigma} = 2S_y \text{ and } (\mathbf{C}^{-1}\boldsymbol{\sigma} + \mathbf{V})^{\mathrm{t}}\mathbf{K}\dot{\boldsymbol{\varepsilon}} > 0, \tag{120}$$

$$\dot{\lambda} = 0 \quad \text{if } \boldsymbol{\sigma}^{\mathrm{t}}\mathbf{C}^{-1}\boldsymbol{\sigma} + 2\mathbf{V}^{\mathrm{t}}\boldsymbol{\sigma} < 2S_y \text{ or } (\mathbf{C}^{-1}\boldsymbol{\sigma} + \mathbf{V})^{\mathrm{t}}\mathbf{K}\dot{\boldsymbol{\varepsilon}} \leqslant 0. \tag{121}$$

Substituting the above $\dot{\lambda}$ into Eq. (119) we obtain the two-phase governing equations:

$$\dot{\boldsymbol{\sigma}} = \mathbf{K}\dot{\boldsymbol{\varepsilon}} - \frac{(\mathbf{C}^{-1}\boldsymbol{\sigma} + \mathbf{V})^{\mathrm{t}}\mathbf{K}\dot{\boldsymbol{\varepsilon}}}{(\mathbf{C}^{-1}\boldsymbol{\sigma} + \mathbf{V})^{\mathrm{t}}\mathbf{K}(\mathbf{C}^{-1}\boldsymbol{\sigma} + \mathbf{V})}\mathbf{K}(\mathbf{C}^{-1}\boldsymbol{\sigma} + \mathbf{V}),$$
$$\text{if } \boldsymbol{\sigma}^{\mathrm{t}}\mathbf{C}^{-1}\boldsymbol{\sigma} + 2\mathbf{V}^{\mathrm{t}}\boldsymbol{\sigma} = 2S_y \text{ and } (\mathbf{C}^{-1}\boldsymbol{\sigma} + \mathbf{V})^{\mathrm{t}}\mathbf{K}\dot{\boldsymbol{\varepsilon}} > 0, \tag{122}$$

$$\dot{\boldsymbol{\sigma}} = \mathbf{K}\dot{\boldsymbol{\varepsilon}}, \quad \text{if } \boldsymbol{\sigma}^{\mathrm{t}}\mathbf{C}^{-1}\boldsymbol{\sigma} + 2\mathbf{V}^{\mathrm{t}}\boldsymbol{\sigma} < 2S_y \text{ or } (\mathbf{C}^{-1}\boldsymbol{\sigma} + \mathbf{V})^{\mathrm{t}}\mathbf{K}\dot{\boldsymbol{\varepsilon}} \leqslant 0. \tag{123}$$

As can be seen the elastic equation is easy to solve; however, the plastic equation is highly non-linear. In the following we are going to reduce the non-linear plastic equation to a quasi-linear one through a group-theoretic approach.

We seek a variable transformation

$$\boldsymbol{\sigma} = \mathbf{T}(\lambda)\boldsymbol{\tau} - \mathbf{C}\mathbf{V}, \tag{124}$$

where $\mathbf{T}(\lambda)$ is an $n \times n$ matrix function of $\lambda$ to be determined below. For this equation we may consider two cases. If $\mathbf{V} = \mathbf{0}$, we just seek the transformation $\boldsymbol{\sigma} = \mathbf{T}(\lambda)\boldsymbol{\tau}$ such that $\boldsymbol{\sigma}$ can be computed from $\boldsymbol{\tau}$ without worrying the property of $\mathbf{C}^{-1}$. However, for the case $\mathbf{V} \neq \mathbf{0}$, the transformation (124) makes sense only if $\mathbf{C}^{-1}$ is not a singular matrix; otherwise, the $\mathbf{C}$ in the above equation cannot be defined. In the below we assume that $\mathbf{C}^{-1}$ is not a singular matrix. However, there are material models whose $\mathbf{C}^{-1}$ are singular. For such cases we can transform Eq. (119) into a suitable stress subspace, such that in this subspace the new $\mathbf{C}^{-1}$ is not singular and the following method is still applicable.

By Eq. (124), Eq. (119) is changed to

$$\dot{\boldsymbol{\tau}} + \dot{\lambda}(\mathbf{T}^{-1}\mathbf{T}' + \mathbf{T}^{-1}\mathbf{K}\mathbf{C}^{-1}\mathbf{T})\boldsymbol{\tau} = \mathbf{T}^{-1}\mathbf{K}\dot{\boldsymbol{\varepsilon}}, \tag{125}$$

where $\mathbf{T}'$ means the differential with respect to $\lambda$. This stimulates us to set

$$\mathbf{T}^{-1}\mathbf{T}' + \mathbf{T}^{-1}\mathbf{K}\mathbf{C}^{-1}\mathbf{T} = \mathbf{I}_n, \tag{126}$$

such that Eq. (125) becomes

$$\dot{\boldsymbol{\tau}} + \dot{\lambda}\boldsymbol{\tau} = \mathbf{T}^{-1}\mathbf{K}\dot{\boldsymbol{\varepsilon}}, \tag{127}$$

where

$$\mathbf{T} = \exp[\lambda(\mathbf{I}_n - \mathbf{K}\mathbf{C}^{-1})] \tag{128}$$

is solved from Eq. (126) by subjecting to $\mathbf{T}(0) = \mathbf{I}_n$.

In terms of $\boldsymbol{\tau}$ the yield condition (8) can be written as

$$\boldsymbol{\tau}^{\mathrm{t}}\mathbf{T}^{\mathrm{t}}\mathbf{C}^{-1}\mathbf{T}\boldsymbol{\tau} = q_y^2 \tag{129}$$

via the map (124) with $\mathbf{T}$ given by Eq. (128), and also the $\dot{\lambda}$ in Eq. (120) can be expressed by

$$\dot{\lambda} = \frac{\boldsymbol{\tau}^{\mathrm{t}}\mathbf{T}^{\mathrm{t}}\mathbf{C}^{-1}\mathbf{K}\dot{\boldsymbol{\varepsilon}}}{\boldsymbol{\tau}^{\mathrm{t}}\mathbf{T}^{\mathrm{t}}\mathbf{C}^{-1}\mathbf{K}\mathbf{C}^{-1}\mathbf{T}\boldsymbol{\tau}}. \tag{130}$$

Let

$$X_0 := \exp\lambda, \tag{131}$$

and thus Eq. (130) can be written as

$$\frac{\dot{X}_0}{X_0}=\frac{\boldsymbol{\tau}^{\mathrm{t}}\mathbf{T}^{\mathrm{t}}\mathbf{C}^{-1}\mathbf{K}\dot{\boldsymbol{\varepsilon}}}{\boldsymbol{\tau}^{\mathrm{t}}\mathbf{T}^{\mathrm{t}}\mathbf{C}^{-1}\mathbf{K}\mathbf{C}^{-1}\mathbf{T}\boldsymbol{\tau}}. \tag{132}$$

As a consequence, Eqs. (127) and (132) can be arranged in the following quasi-linear system:

$$\dot{\mathbf{X}}=\mathbf{A}\mathbf{X}, \tag{133}$$

where

$$\mathbf{X}=\begin{bmatrix}\mathbf{X}_s\\ X_0\end{bmatrix}:=\begin{bmatrix}X_0\boldsymbol{\tau}\\ X_0\end{bmatrix}, \tag{134}$$

and

$$\mathbf{A}:=\begin{bmatrix}\mathbf{0}_n & \mathbf{U}_2\\ \mathbf{U}_1^{\mathrm{t}} & 0\end{bmatrix}=\begin{bmatrix}\mathbf{0}_n & \mathbf{T}^{-1}\mathbf{K}\dot{\boldsymbol{\varepsilon}}\\ \frac{X_0^2\dot{\boldsymbol{\varepsilon}}^{\mathrm{t}}\mathbf{K}\mathbf{C}^{-1}\mathbf{T}}{\mathbf{X}_s^{\mathrm{t}}\mathbf{T}^{\mathrm{t}}\mathbf{C}^{-1}\mathbf{K}\mathbf{C}^{-1}\mathbf{T}\mathbf{X}_s} & 0\end{bmatrix}=\begin{bmatrix}\mathbf{0}_n & \mathbf{T}^{-1}\mathbf{K}\dot{\boldsymbol{\varepsilon}}\\ \frac{\dot{\boldsymbol{\varepsilon}}^{\mathrm{t}}\mathbf{K}\mathbf{C}^{-1}\mathbf{T}}{\boldsymbol{\tau}^{\mathrm{t}}\mathbf{T}^{\mathrm{t}}\mathbf{C}^{-1}\mathbf{K}\mathbf{C}^{-1}\mathbf{T}\boldsymbol{\tau}} & 0\end{bmatrix} \tag{135}$$

is really an element of the Lie algebra of the special orthochronous pseudo-linear group $\mathrm{SL}(n,1,\mathbb{R})$, namely $\mathbf{A}\in\mathrm{sl}(n,1,\mathbb{R})$. From Eqs. (129) and (134) it follows that

$$\mathbf{X}^{\mathrm{t}}\mathbf{g}\mathbf{X}=0, \tag{136}$$

where

$$\mathbf{g}:=\begin{bmatrix}\mathbf{T}^{\mathrm{t}}\mathbf{C}^{-1}\mathbf{T} & \mathbf{0}\\ \mathbf{0} & -q_y^2\end{bmatrix} \tag{137}$$

is an indefinite metric. The pseudo-Riemann manifold endowed with a metric tensor $\mathbf{g}$ dependent on the temporal component $X_0$ is known as the Robertson–Walker space in the special relativity theory; see Liu (2003a, 2004c). Eq. (136) signifies an elliptical cone in the space $\mathbf{X}$.

## 9. Numerical method for the anisotropic quadratic yielding model

The effective utilization of the time invariance property of plasticity models will help to capture the key qualitative features, enhance the long-term numerical stability, and much improve efficiency and accuracy. Hence, we would like to call the attention to its importance in the computation, except in a very few cases where the exact solutions are available, by developing a group-preserving and consistent numerical scheme for the anisotropic quadratic yielding model.

### 9.1. The Cayley transform

In order to develop a numerical method for the anisotropic quadratic yielding model, let us first prove that the Cayley transform

$$\mathrm{Cay}(\tau\mathbf{A}):=(\mathbf{I}_{n+1}-\tau\mathbf{A})^{-1}(\mathbf{I}_{n+1}+\tau\mathbf{A}) \tag{138}$$

gives us a $\mathrm{SL}(n+1,\mathbb{R})$ group-preserving transformation for system (133). In above, $\tau>0$ is a real scalar.

For the $\mathbf{A}$ given by Eq. (135) through a lengthy calculation we can derive the following eigen-formula:

$$\det(\mathbf{A}-\lambda\mathbf{I}_{n+1})=(-1)^{n+1}[\lambda^{n+1}-\mathbf{U}_1^{\mathrm{t}}\mathbf{U}_2\lambda^{n-1}]. \tag{139}$$

Thus, we have

$$\det(\mathrm{Cay}(\tau\mathbf{A})) = \det[(\mathbf{I}_{n+1}-\tau\mathbf{A})^{-1}(\mathbf{I}_{n+1}+\tau\mathbf{A})] = \frac{\det(\mathbf{I}_{n+1}+\tau\mathbf{A})}{\det(\mathbf{I}_{n+1}-\tau\mathbf{A})} = \frac{\det(\tau\mathbf{I}_{n+1})\det(\mathbf{A}+\frac{1}{\tau}\mathbf{I}_{n+1})}{\det(-\tau\mathbf{I}_{n+1})\det(\mathbf{A}-\frac{1}{\tau}\mathbf{I}_{n+1})}$$
$$= \frac{(-1)^{n+1}\det(\mathbf{A}+\frac{1}{\tau}\mathbf{I}_{n+1})}{\det(\mathbf{A}-\frac{1}{\tau}\mathbf{I}_{n+1})}, \tag{140}$$

which leads to, by means of Eq. (139),

$$\det(\mathrm{Cay}(\tau\mathbf{A})) = \frac{(-1)^{n+1}[(\frac{-1}{\tau})^{n+1}-(\frac{-1}{\tau})^{n-1}\mathbf{U}_1^{\mathrm{t}}\mathbf{U}_2]}{(\frac{1}{\tau})^{n+1}-(\frac{1}{\tau})^{n-1}\mathbf{U}_1^{\mathrm{t}}\mathbf{U}_2} = 1. \tag{141}$$

That is, the Cayley transform preserves the special linear group property, i.e., $\mathrm{Cay}(\tau\mathbf{A}) \in \mathrm{SL}(n,1,\mathbb{R})$.

In terms of the Cayley transform the following numerical scheme for system (133) is available:

$$\mathbf{X}(\ell+1) = \mathrm{Cay}(\tau\mathbf{A}(\ell))\mathbf{X}(\ell) = [\mathbf{I}_{n+1}-\tau\mathbf{A}(\ell)]^{-1}[\mathbf{I}_{n+1}+\tau\mathbf{A}(\ell)]\mathbf{X}(\ell), \tag{142}$$

where $\mathbf{X}(\ell)$ denotes the numerical value of $\mathbf{X}$ at a discrete time step $t_\ell$, $\mathbf{A}(\ell) := \mathbf{A}(t_\ell)$, and $\tau$ is one half of the time increment, $\tau := \Delta t/2 = (t_{\ell+1}-t_\ell)/2$. Let us recall that

$$\begin{bmatrix}\mathbf{I}_n & \mathbf{b}\\ \mathbf{a}^{\mathrm{t}} & 1\end{bmatrix}^{-1} = \frac{1}{1-\mathbf{a}^{\mathrm{t}}\mathbf{b}}\begin{bmatrix}(1-\mathbf{a}^{\mathrm{t}}\mathbf{b})\mathbf{I}_n+\mathbf{b}\mathbf{a}^{\mathrm{t}} & -\mathbf{b}\\ -\mathbf{a}^{\mathrm{t}} & 1\end{bmatrix} \tag{143}$$

for arbitrary $n$-dimensional vectors $\mathbf{a}$ and $\mathbf{b}$ with $\mathbf{a}^{\mathrm{t}}\mathbf{b} \neq 1$. From the above equation it follows that

$$[\mathbf{I}_{n+1}-\tau\mathbf{A}(\ell)]^{-1} = \begin{bmatrix}\mathbf{I}_n+\frac{\tau^2\mathbf{U}_2(\ell)\mathbf{U}_1^{\mathrm{t}}(\ell)}{1-\tau^2\mathbf{U}_1^{\mathrm{t}}(\ell)\mathbf{U}_2(\ell)} & \frac{\tau\mathbf{U}_2(\ell)}{1-\tau^2\mathbf{U}_1^{\mathrm{t}}(\ell)\mathbf{U}_2(\ell)}\\ \frac{\tau\mathbf{U}_1^{\mathrm{t}}(\ell)}{1-\tau^2\mathbf{U}_1^{\mathrm{t}}(\ell)\mathbf{U}_2(\ell)} & \frac{1}{1-\tau^2\mathbf{U}_1^{\mathrm{t}}(\ell)\mathbf{U}_2(\ell)}\end{bmatrix}. \tag{144}$$

Through some calculations we thus obtain

$$\mathrm{Cay}(\tau\mathbf{A}(\ell)) = \begin{bmatrix}\mathbf{I}_n+\frac{2\tau^2\mathbf{U}_2(\ell)\mathbf{U}_1^{\mathrm{t}}(\ell)}{1-\tau^2\mathbf{U}_1^{\mathrm{t}}(\ell)\mathbf{U}_2(\ell)} & \frac{2\tau\mathbf{U}_2(\ell)}{1-\tau^2\mathbf{U}_1^{\mathrm{t}}(\ell)\mathbf{U}_2(\ell)}\\ \frac{2\tau\mathbf{U}_1^{\mathrm{t}}(\ell)}{1-\tau^2\mathbf{U}_1^{\mathrm{t}}(\ell)\mathbf{U}_2(\ell)} & \frac{1+\tau^2\mathbf{U}_1^{\mathrm{t}}(\ell)\mathbf{U}_2(\ell)}{1-\tau^2\mathbf{U}_1^{\mathrm{t}}(\ell)\mathbf{U}_2(\ell)}\end{bmatrix}. \tag{145}$$

Substituting it into (142) we obtain a numerical solution for system (133). Then, by means of Eq. (134) we can calculate $\boldsymbol{\tau}$ forward step-by-step.

From Eqs. (134), (142) and (145) we get

$$\begin{bmatrix}X_0(\ell+1)\boldsymbol{\tau}(\ell+1)\\ X_0(\ell+1)\end{bmatrix} = \begin{bmatrix}\mathbf{I}_n+\frac{2\tau^2\mathbf{U}_2(\ell)\mathbf{U}_1^{\mathrm{t}}(\ell)}{1-\tau^2\mathbf{U}_1^{\mathrm{t}}(\ell)\mathbf{U}_2(\ell)} & \frac{2\tau\mathbf{U}_2(\ell)}{1-\tau^2\mathbf{U}_1^{\mathrm{t}}(\ell)\mathbf{U}_2(\ell)}\\ \frac{2\tau\mathbf{U}_1^{\mathrm{t}}(\ell)}{1-\tau^2\mathbf{U}_1^{\mathrm{t}}(\ell)\mathbf{U}_2(\ell)} & \frac{1+\tau^2\mathbf{U}_1^{\mathrm{t}}(\ell)\mathbf{U}_2(\ell)}{1-\tau^2\mathbf{U}_1^{\mathrm{t}}(\ell)\mathbf{U}_2(\ell)}\end{bmatrix}\begin{bmatrix}X_0(\ell)\boldsymbol{\tau}(\ell)\\ X_0(\ell)\end{bmatrix}. \tag{146}$$

Dividing the first row by the second row we obtain

$$\boldsymbol{\tau}(\ell+1) = \frac{1}{S_2(\ell)}\{[S_1(\ell)\mathbf{I}_n+2\tau^2\mathbf{U}_2(\ell)\mathbf{U}_1^{\mathrm{t}}(\ell)]\boldsymbol{\tau}(\ell)+2\tau\mathbf{U}_2(\ell)\}. \tag{147}$$

On the other hand, by taking the second row of Eq. (146) we get

$$X_0(\ell+1) = X_0(\ell)\frac{S_2(\ell)}{S_1(\ell)}, \tag{148}$$

where

$$S_1(\ell) := 1-\tau^2\mathbf{U}_1^{\mathrm{t}}(\ell)\mathbf{U}_2(\ell), \tag{149}$$

$$S_2(\ell) := 1 + \tau^2 \mathbf{U}_1^{\mathrm{t}}(\ell)\mathbf{U}_2(\ell) + 2\tau \mathbf{U}_1^{\mathrm{t}}(\ell)\boldsymbol{\tau}(\ell). \tag{150}$$

In terms of $\lambda$ by Eq. (131) we thus obtain

$$\lambda(\ell+1) = \lambda(\ell) + \ln\frac{S_2(\ell)}{S_1(\ell)}. \tag{151}$$

The numerical schemes (147) and (151) can be re-expressed in terms of $\boldsymbol{\sigma}$ by the transform (124):

$$\boldsymbol{\sigma}(\ell+1) = \frac{\mathbf{J}(\ell)}{S_2(\ell)} - \mathbf{C}\mathbf{V}, \tag{152}$$

where

$$S_1(\ell) := 1 - \tau^2 \mathbf{U}_3^{\mathrm{t}}(\ell)\mathbf{K}\dot{\boldsymbol{\varepsilon}}(\ell), \tag{153}$$

$$S_2(\ell) := 2 - S_1(\ell) + 2\tau \mathbf{U}_3^{\mathrm{t}}(\ell)[\boldsymbol{\sigma}(\ell) + \mathbf{C}\mathbf{V}], \tag{154}$$

$$\mathbf{J}(\ell) = \mathbf{J}_1(\ell) + \mathbf{J}_2(\ell) + \mathbf{J}_3(\ell), \tag{155}$$

$$\mathbf{J}_1(\ell) = S_1(\ell)\mathbf{T}(\Delta\lambda(\ell))[\boldsymbol{\sigma}(\ell) + \mathbf{C}\mathbf{V}], \tag{156}$$

$$\mathbf{J}_2(\ell) = 2\tau^2 \mathbf{T}(\Delta\lambda(\ell))\mathbf{K}\dot{\boldsymbol{\varepsilon}}(\ell)\mathbf{U}_3^{\mathrm{t}}(\ell)[\boldsymbol{\sigma}(\ell) + \mathbf{C}\mathbf{V}], \tag{157}$$

$$\mathbf{J}_3(\ell) = 2\tau \mathbf{T}(\Delta\lambda(\ell))\mathbf{K}\dot{\boldsymbol{\varepsilon}}(\ell), \tag{158}$$

in which $\mathbf{U}_3$ is a new vector defined by

$$\mathbf{U}_3(\ell) := \frac{\mathbf{C}^{-1}\mathbf{K}\dot{\boldsymbol{\varepsilon}}(\ell)}{[\mathbf{C}^{-1}\boldsymbol{\sigma}(\ell) + \mathbf{V}]^{\mathrm{t}}\mathbf{K}[\mathbf{C}^{-1}\boldsymbol{\sigma}(\ell) + \mathbf{V}]}. \tag{159}$$

The matrix term $\mathbf{T}(\Delta\lambda)$ in Eqs. (156)–(158) can be calculated by the precise integral method of Zhong (1994). Denoting the matrix $\mathbf{H} := \mathbf{I}_n - \mathbf{K}\mathbf{C}^{-1}$, the integration of $\mathbf{T}(\Delta\lambda) = \exp(\Delta\lambda\mathbf{H})$ is using a subincrement to increase the accuracy:

$$\exp(\Delta\lambda\mathbf{H}) = [\exp(\Delta\lambda/m\mathbf{H})]^m, \tag{160}$$

where $m = 2^p$; for example for $p = 20$ we have $m = 1\,048\,576$. In doing so $\Delta\lambda/m$ will be a very small increment, and thus

$$\exp(\Delta\lambda/m\mathbf{H}) \approx \mathbf{I}_n + \mathbf{T}_a := \mathbf{I}_n + \Delta\lambda/m\mathbf{H} + (\Delta\lambda/m\mathbf{H})^2[\mathbf{I}_n + (\Delta\lambda/m\mathbf{H})/3 + (\Delta\lambda/m\mathbf{H})^2/12]/2 \tag{161}$$

would have the accuracy in the order of $(\Delta\lambda/m)^4$. By performing the decomposition

$$\exp(\Delta\lambda\mathbf{H}) \approx [\mathbf{I}_n + \mathbf{T}_a]^{2^p} = [\mathbf{I}_n + \mathbf{T}_a]^{2^{(p-1)}}[\mathbf{I}_n + \mathbf{T}_a]^{2^{(p-1)}}, \tag{162}$$

and repeating it $p$ times we obtain $\exp(\Delta\lambda\mathbf{H})$. Then we can perform the following iterations to compute $\mathbf{T}(\Delta\lambda)$:

$$\text{for} \quad (\text{iter} = 0; \text{iter} < p; \text{iter}++)\mathbf{T}_a = 2\mathbf{T}_a + \mathbf{T}_a\mathbf{T}_a. \tag{163}$$

When the circulation is ended we get

$$\mathbf{T}(\Delta\lambda) = \mathbf{I}_n + \mathbf{T}_a. \tag{164}$$

The above Eqs. (151)–(164) can be used to calculate the stress step-by-step forward. However, in order to match the consistency condition during the plastic loading phase we can insert Eq. (152) for $\boldsymbol{\sigma}$ into the yield condition (29), and solve it for $S_2(\ell)$ to obtain

$$S_2(\ell)=\sqrt{\frac{\mathbf{J}^{\mathrm{t}}(\ell+1)\mathbf{C}^{-1}\mathbf{J}(\ell+1)}{q_y^2}}. \tag{165}$$

With this new value of $S_2(\ell)$ which being inserted into Eq. (152) we obtain a stress $\boldsymbol{\sigma}$ which is exactly located on the yield surface. On the other hand by Eq. (151) we obtain a new $\lambda$, and from which the increment $\Delta\lambda(\ell)=\lambda(\ell+1)-\lambda(\ell)$ can be updated. In Fig. 4 we display the numerical procedures to update the stress by enforcing the consistency condition.

Even the numerical implementation of these integration techniques into the commercial programs with FE-code, such as ABAQUS, is not carried out here, we can expect that this study provides not only a deeper understanding of the mathematical structures of the plastic flow model with the anisotropic tensors $\mathbf{K}$ and $\mathbf{C}^{-1}$, but also the foundation of numerical solutions for the non-linear problems of plasticity. Given $\mathbf{K}$, $\mathbf{C}^{-1}$, $\mathbf{V}$ and $S_y$ the coefficients in the algorithms Eqs. (151)–(165) under a strain-driven program can be calculated directly since they were derived explicitly, such that only a few simple calculations are needed in the numerical implementation of the FE-code.

### 9.2. Numerical result for the Drucker–Prager yield model

For the case of $\mathbf{C}^{-1}$ non-positive or $q_y=0$ the modification (165) is not applicable. However, we can still apply the algorithms (151)–(164) to this case, to be shown below for the Drucker–Prager yield model as an example.

For simplicity we consider an isotropic elastic law with

$$\mathbf{K}=\begin{bmatrix} \frac{2\mu(1-\nu)}{1-2\nu} & \frac{2\mu\nu}{1-2\nu} & \frac{2\mu\nu}{1-2\nu} & 0 & 0 & 0\\ \frac{2\mu\nu}{1-2\nu} & \frac{2\mu(1-\nu)}{1-2\nu} & \frac{2\mu\nu}{1-2\nu} & 0 & 0 & 0\\ \frac{2\mu\nu}{1-2\nu} & \frac{2\mu\nu}{1-2\nu} & \frac{2\mu(1-\nu)}{1-2\nu} & 0 & 0 & 0\\ 0 & 0 & 0 & 2\mu & 0 & 0\\ 0 & 0 & 0 & 0 & 2\mu & 0\\ 0 & 0 & 0 & 0 & 0 & 2\mu \end{bmatrix}, \tag{166}$$

where $\mu$ is the shear modulus and $\nu$ is the Poisson ratio. Corresponding to the $\mathbf{C}^{-1}$ given in Eq. (10) for the Drucker–Prager model, the $\mathbf{C}$ is found to be

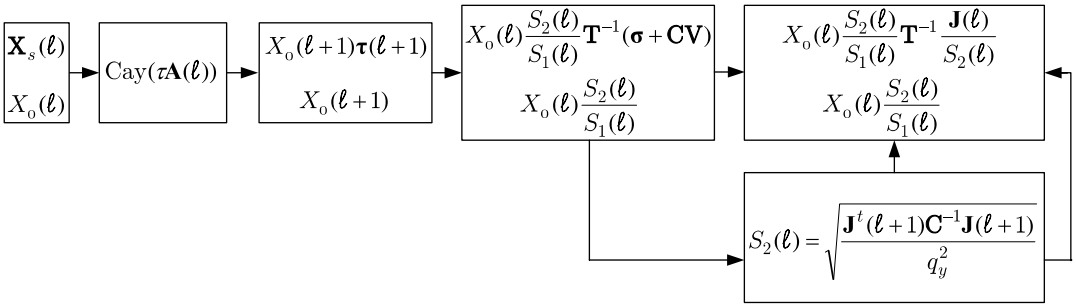


Fig. 4. A numerical procedure to enhance the consistent condition.

$$\mathbf{C}=\begin{bmatrix} \frac{12\alpha^2-1}{27\alpha^2} & -\frac{6\alpha^2+1}{27\alpha^2} & -\frac{6\alpha^2+1}{27\alpha^2} & 0 & 0 & 0 \\ -\frac{6\alpha^2+1}{27\alpha^2} & \frac{12\alpha^2-1}{27\alpha^2} & -\frac{6\alpha^2+1}{27\alpha^2} & 0 & 0 & 0 \\ -\frac{6\alpha^2+1}{27\alpha^2} & -\frac{6\alpha^2+1}{27\alpha^2} & \frac{12\alpha^2-1}{27\alpha^2} & 0 & 0 & 0 \\ 0 & 0 & 0 & \frac{1}{3} & 0 & 0 \\ 0 & 0 & 0 & 0 & \frac{1}{3} & 0 \\ 0 & 0 & 0 & 0 & 0 & \frac{1}{3} \end{bmatrix}. \tag{167}$$

By using the above $\mathbf{K}$, $\mathbf{C}$ and $\mathbf{C}^{-1}$ and $\mathbf{V}$ in Eq. (10) we can calculate the responses by Eqs. (151)–(164). However, for the Drucker–Prager model $\mathbf{C}^{-1}$ is non-positive definite, and we have $q_y = 0$ by Eqs. (48), (10) and (166), and hence the modification (165) is not applicable for this model.

Before that we need to determine the switch-on time under a rectilinear strain path with constant strain rate. Substituting the elastic equation (99) into the yield condition (8) we obtain a quadratic equation for $t - t_1$:

$$A(t-t_1)^2 + B(t-t_1) + C = 0, \tag{168}$$

where

$$A = \dot{\boldsymbol{\varepsilon}}^{\mathrm{t}}\mathbf{K}\mathbf{C}^{-1}\mathbf{K}\dot{\boldsymbol{\varepsilon}},$$

$$B := 2\dot{\boldsymbol{\varepsilon}}^{\mathrm{t}}\mathbf{K}\mathbf{C}^{-1}\boldsymbol{\sigma}(t_1) + 2\dot{\boldsymbol{\varepsilon}}^{\mathrm{t}}\mathbf{K}\mathbf{V},$$

$$C := \boldsymbol{\sigma}^{\mathrm{t}}(t_1)\mathbf{C}^{-1}\boldsymbol{\sigma}(t_1) + 2\mathbf{V}^{\mathrm{t}}\boldsymbol{\sigma}(t_1) - 2S_y.$$

Since $\mathbf{C}^{-1}$ is not positive definite, we should consider three possible cases: $A > 0$, $A = 0$ and $A < 0$. If $A > 0$, we have

$$t_{\mathrm{on}} = \begin{cases} t_1 & \text{if } C = 0 \text{ and } B \geqslant 0, \\ t_1 - \frac{B}{A} & \text{if } C = 0 \text{ and } B < 0, \\ t_1 + \frac{\sqrt{B^2-4AC}-B}{2A} & \text{if } C < 0. \end{cases} \tag{169}$$

If $A = 0$, we have

$$t_{\mathrm{on}} = t_1 - \frac{C}{B}. \tag{170}$$

If $A < 0$, we have

$$t_{\mathrm{on}} = \begin{cases} t_1 & \text{if } C = 0 \text{ and } B \geqslant 0, \\ t_1 + \frac{B}{A} & \text{if } C = 0 \text{ and } B < 0, \\ t_{y1} & \text{if } C < 0 \text{ and } t_{y1} \geqslant t_1, \\ t_{y2} & \text{if } C < 0 \text{ and } t_{y1} < t_1, \end{cases} \tag{171}$$

where

$$t_{y1} := t_1 + \frac{\sqrt{B^2-4AC}-B}{2A}, \qquad t_{y2} := t_1 - \frac{\sqrt{B^2-4AC}+B}{2A},$$

and $t_{y1} \leqslant t_{y2}$.

Now, let us apply the above scheme to a certain example. The material constants used in the calculation were $\mu = 20.67\,\text{MPa}$, $v = 0.3$, $\tau_y = 0.14848\,\text{MPa}$ and $\alpha = 0.2$. Fig. 5 displays a rectangular strain path, the corresponding stress path and the stress–strain curves in the axial and torsional directions under two cycles of the strain inputs. In Fig. 5(e) we show the consistency error defined by $\boldsymbol{\sigma}^{\mathrm{t}}\mathbf{C}^{-1}\boldsymbol{\sigma} + 2\mathbf{V}^{\mathrm{t}}\boldsymbol{\sigma} - 2S_y$, which as

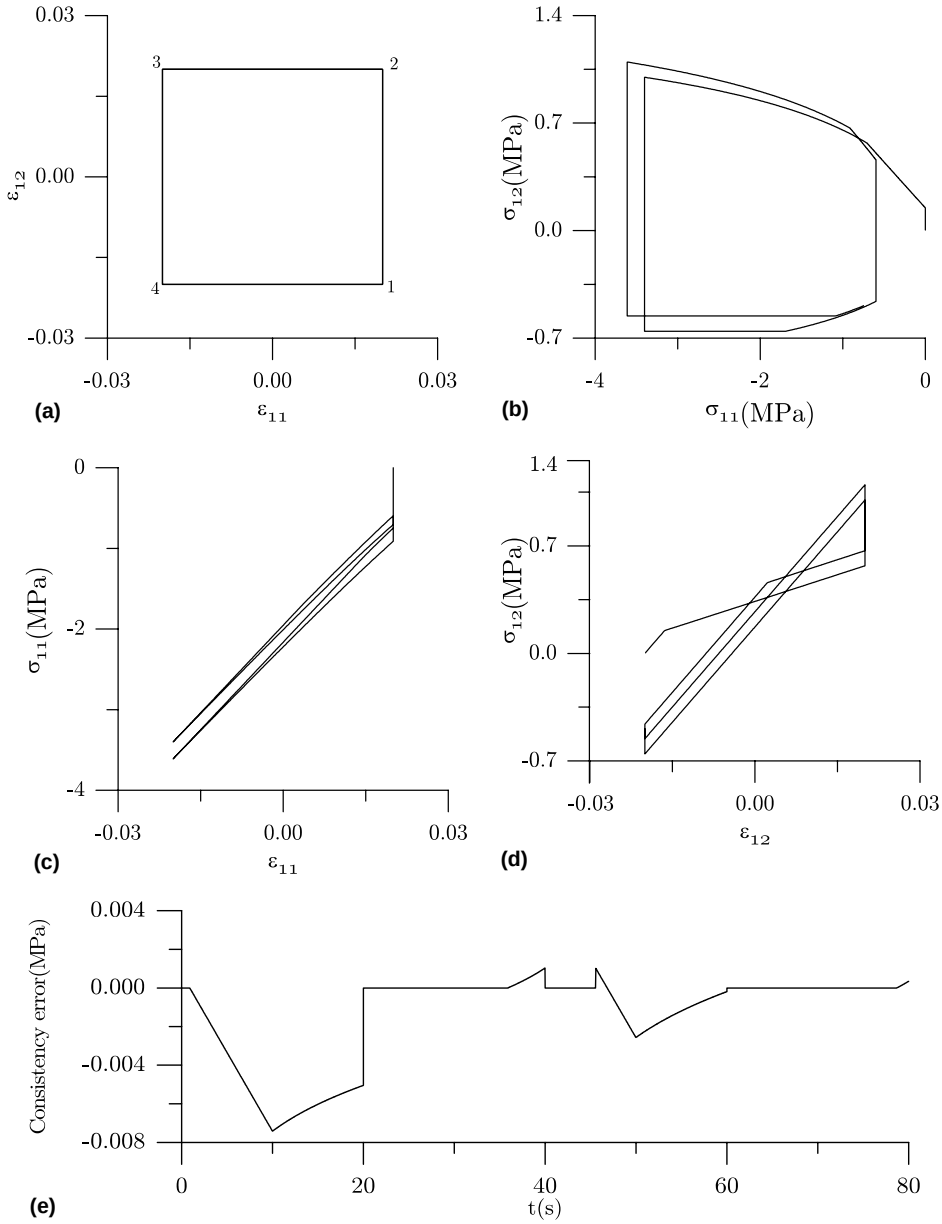


Fig. 5. The responses of Drucker–Prager model to an input of cyclic square strain path in (a), and (b) displaying its corresponding stress path, (c) the cyclic axial stress–axial strain curve, (d) the cyclic shear stress–shear strain curve, and (e) the consistency error.

can be seen is small, but is not zero exactly. In the paper by Liu (2004c), some consistent schemes are available for the Drucker–Prager model but by another approaches.

### 9.3. Numerical result for the Hill yield model

As mentioned in Section 1 the $\mathbf{C}^{-1}$ as given in Eq. (11) for the Hill yield criterion is a singular matrix. Therefore, the numerical method developed in Section 9.1 seems not applicable. However this is not true, since $\mathbf{V}$ for the Hill model is zero, and for such case we do not need $\mathbf{C}$ in Eqs. (151)–(165). Below, we solve the numerical integration problem of Hill model with the yield criterion (4) by expressing it in terms of the deviatoric stresses:

$$F(s_{22}-s_{33})^2+G(s_{33}-s_{11})^2+H(s_{11}-s_{22})^2+2Ls_{23}^2+2Ms_{13}^2+2Ns_{12}^2=1, \tag{172}$$

which by $s_{33}=-s_{11}-s_{22}$ can be rearranged to

$$(H+F+4G)s_{11}^2+(H+G+4F)s_{22}^2+2(2G+2F-H)s_{11}s_{22}+2Ls_{23}^2+2Ms_{13}^2+2Ns_{12}^2=1. \tag{173}$$

Thus, in the five-dimensional deviatoric stress space we have Eq. (8) with the followings

$$\mathbf{C}^{-1}=\begin{bmatrix} H+F+4G & 2G+2F-H & 0 & 0 & 0\\ 2G+2F-H & H+G+4F & 0 & 0 & 0\\ 0 & 0 & 2L & 0 & 0\\ 0 & 0 & 0 & 2M & 0\\ 0 & 0 & 0 & 0 & 2N \end{bmatrix},\qquad \boldsymbol{\sigma}=\begin{bmatrix} s_{11}\\ s_{22}\\ s_{23}\\ s_{13}\\ s_{12}\end{bmatrix}, \tag{174}$$

and $\mathbf{V}=\mathbf{0}$ and $S_y=1/2$. Obviously, the above $\mathbf{C}^{-1}$ is positive definite with the eigenvalues $[2H+5G+5F\pm(4H^2+25G^2+25F^2-16HG-16HF+14GF)^{1/2}]/2$, $2L$, $2M$ and $2N$ all positive. By using the $\mathbf{C}^{-1}$ in Eq. (174) and $\mathbf{K}=2\mu\mathbf{I}_5$ we can calculate the responses by Eqs. (151)–(165).

When applying the above scheme to the Hill model we fix the parameters to be $F=1.535\times10^{-5}\,1/\mathrm{MPa}^2$, $G=1.029\times10^{-5}\,1/\mathrm{MPa}^2$, $H=1.711\times10^{-5}\,1/\mathrm{MPa}^2$, $L=4.305\times10^{-5}\,1/\mathrm{MPa}^2$, $M=3.305\times10^{-5}\,1/\mathrm{MPa}^2$, $N=5.704\times10^{-5}\,1/\mathrm{MPa}^2$ and $\mu=5000\,\mathrm{MPa}$. Fig. 6 displays a rectangular strain path, the corresponding stress path and the stress–strain curves in the axial and torsional directions under two cycles of the strain inputs.

## 10. Concluding remarks

In order to give a unified treatment of the material plastic models with the yield criterion based on the quadratic yield function, we divided them into two types: strain-energy yielding model and anisotropic quadratic yielding model.

For the first type of the models the elastic tensor $\mathbf{K}$ in the rate equation $\dot{\boldsymbol{\sigma}}=\mathbf{K}\dot{\boldsymbol{\varepsilon}}$ is also the anisotropic tensor in the quadratic yield criterion: $\boldsymbol{\sigma}^{\mathrm{t}}\mathbf{K}^{-1}\boldsymbol{\sigma}+2\mathbf{V}^{\mathrm{t}}\boldsymbol{\sigma}=2S_y$. We have proved that the plastic equation can be linearized in a non-canonical Minkowski space, of which the symmetry group is a special orthochronous pseudo-linear group $\mathrm{SL}(n,1,\mathbb{R})$. However, we proposed two approaches to reveal its canonical Minkowski structure, of which the plastic equation exhibits the proper orthochronous Lorentz group symmetry $\mathrm{SO}_{\mathrm{o}}(n,1)$. Numerical examples were given under strain controls and stress controls. For the latter case a varying smoothing factor was used to reveal the ratcheting behavior with a decreasing rate per cycle and a saturation of strain.

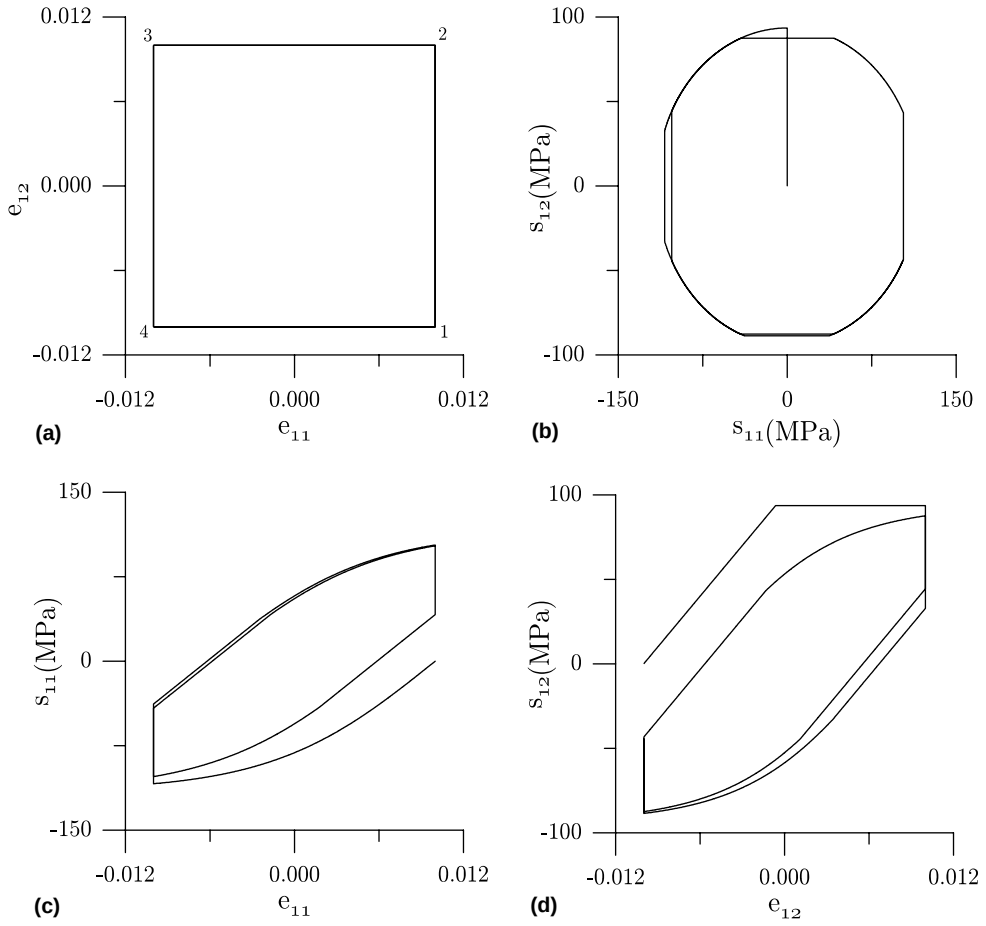


Fig. 6. The responses of Hill model to an input of cyclic square strain path in (a), and (b) displaying its corresponding stress path, (c) the cyclic $(e_{11},s_{11})$ curve, and (d) the cyclic $(e_{12},s_{12})$ curve.

Then, we consider the anisotropic quadratic yielding model with $\boldsymbol{\sigma}^{\mathrm{t}}\mathbf{C}^{-1}\boldsymbol{\sigma}+2\mathbf{V}^{\mathrm{t}}\boldsymbol{\sigma}=2S_y$ by allowing the $\mathbf{C}^{-1}$ to be positive, non-positive or even singular. The non-linear constitutive equations have been converted to a Lie system $\dot{\mathbf{X}}=\mathbf{A}(\mathbf{X},t)\mathbf{X}$ on a pseudo-Riemann manifold, where $\mathbf{A}\in \mathrm{sl}(n,1,\mathbb{R})$ is a Lie algebra of the special orthochronous pseudo-linear group $\mathrm{SL}(n,1,\mathbb{R})$. The underlying space in the plastic phase is a cone with the metric tensor indefinite having a signature $(n,1)$ and also dependent on the temporal component. We proved that the Cayley transform is a Lie integrator preserving $\mathrm{SL}(n,1,\mathbb{R})$, and a consistent numerical scheme was developed to calculate the stress responses.

## Acknowledgment

The financial support provided by the National Science Council under Grants NSC 92-2212-E-019-006 and NSC 93-2212-E-019-008 is gratefully acknowledged.

## Appendix A. The derivation of Eq. (61)

From Eq. (54) it follows that

$$\mathbf{K}^{-1}\frac{\mathrm{d}}{\mathrm{d}t}(\mathscr{X}_0\boldsymbol{\sigma})+\mathbf{V}\dot{\mathscr{X}}_0=\mathscr{X}_0\dot{\boldsymbol{\varepsilon}}. \tag{A.1}$$

Taking the inner product of Eq. (A.1) with **KV** gives

$$\mathbf{V}^{\mathrm{t}}\frac{\mathrm{d}}{\mathrm{d}t}(\mathscr{X}_0\boldsymbol{\sigma})+\mathbf{V}^{\mathrm{t}}\mathbf{K}\mathbf{V}\dot{\mathscr{X}}_0=\mathscr{X}_0\mathbf{V}^{\mathrm{t}}\mathbf{K}\dot{\boldsymbol{\varepsilon}}. \tag{A.2}$$

Substracting it with $2S_y\dot{\mathscr{X}}_0$, leads to

$$\mathbf{V}^{\mathrm{t}}\frac{\mathrm{d}}{\mathrm{d}t}(\mathscr{X}_0\boldsymbol{\sigma})-2S_y\dot{\mathscr{X}}_0=\mathscr{X}_0\mathbf{V}^{\mathrm{t}}\mathbf{K}\dot{\boldsymbol{\varepsilon}}-(\mathbf{V}^{\mathrm{t}}\mathbf{K}\mathbf{V}\dot{\mathscr{X}}_0+2S_y\dot{\mathscr{X}}_0). \tag{A.3}$$

On the other hand, from Eq. (55) by inserting Eq. (48) for $q_y$ it follows that

$$\mathbf{V}^{\mathrm{t}}\mathbf{K}\mathbf{V}\dot{\mathscr{X}}_0+2S_y\dot{\mathscr{X}}_0=\mathscr{X}_0\dot{\boldsymbol{\varepsilon}}^{\mathrm{t}}\boldsymbol{\sigma}+\mathscr{X}_0\mathbf{V}^{\mathrm{t}}\mathbf{K}\dot{\boldsymbol{\varepsilon}}. \tag{A.4}$$

Substituting it for the last two quantities in Eq. (A.3) we obtain

$$\mathbf{V}^{\mathrm{t}}\frac{\mathrm{d}}{\mathrm{d}t}(\mathscr{X}_0\boldsymbol{\sigma})-2S_y\dot{\mathscr{X}}_0=-\dot{\boldsymbol{\varepsilon}}^{\mathrm{t}}\boldsymbol{\sigma}\mathscr{X}_0. \tag{A.5}$$

We can combine Eqs. (A.1) and (A.5) into a single Eq. (61).

## Appendix B. Another approach to the canonical form

In this appendix we propose another approach to the canonical form. The yield criterion (29) can also be written as

$$[\boldsymbol{\sigma}+\mathbf{K}\mathbf{V}]^{\mathrm{t}}\mathbf{K}^{-1}[\boldsymbol{\sigma}+\mathbf{K}\mathbf{V}]=q_y^2, \tag{B.1}$$

where $q_y$ was defined by Eq. (48). This motivates us to define

$$\boldsymbol{\tau}:=\boldsymbol{\sigma}+\mathbf{K}\mathbf{V}, \tag{B.2}$$

and write the yield condition to be

$$\boldsymbol{\tau}^{\mathrm{t}}\mathbf{K}^{-1}\boldsymbol{\tau}=q_y^2. \tag{B.3}$$

At the same time, from Eqs. (B.2) and (41) it follows that

$$\dot{\boldsymbol{\tau}}+\dot{\lambda}\boldsymbol{\tau}=\mathbf{K}\dot{\boldsymbol{\varepsilon}}. \tag{B.4}$$

The above equation together with Eq. (B.3) lead to

$$\dot{\lambda}=\frac{\boldsymbol{\tau}^{\mathrm{t}}\dot{\boldsymbol{\varepsilon}}}{q_y^2}. \tag{B.5}$$

Upon letting

$$\mathscr{Y}_0:=\mathscr{X}_0:=\exp\lambda, \tag{B.6}$$

Eq. (B.5) can be written as

$$\frac{\dot{\mathscr{y}}_0}{\mathscr{y}_0} = \frac{\boldsymbol{\tau}^{\mathrm{t}}\dot{\boldsymbol{\varepsilon}}}{q_y^2}. \tag{B.7}$$

As a consequence, Eqs. (B.4) and (B.7) can be arranged in the following system:

$$\dot{\boldsymbol{\mathscr{y}}} = \mathbf{B}\boldsymbol{\mathscr{y}}, \tag{B.8}$$

where

$$\boldsymbol{\mathscr{y}} = \begin{bmatrix} \boldsymbol{\mathscr{y}}_s \\ \mathscr{y}_0 \end{bmatrix} := \begin{bmatrix} \mathscr{y}_0\boldsymbol{\tau} \\ \mathscr{y}_0 \end{bmatrix}, \tag{B.9}$$

and

$$\mathbf{B} := \begin{bmatrix} \mathbf{0}_n & \mathbf{K}\dot{\boldsymbol{\varepsilon}} \\ q_y^{-2}\dot{\boldsymbol{\varepsilon}}^{\mathrm{t}} & 0 \end{bmatrix} \tag{B.10}$$

is really an element of the Lie algebra of the special orthochronous pseudo-linear group $\mathrm{SL}(n,1,\mathbb{R})$, namely $\mathbf{B} \in \mathrm{sl}(n,1,\mathbb{R})$. Eq. (B.8) is much simpler than that in Eq. (68). From Eqs. (B.3) and (B.9) it follows that

$$\boldsymbol{\mathscr{y}}^{\mathrm{t}}\boldsymbol{\eta}\boldsymbol{\mathscr{y}} = 0, \tag{B.11}$$

where

$$\boldsymbol{\eta} := \begin{bmatrix} \mathbf{K}^{-1} & \mathbf{0} \\ \mathbf{0} & -q_y^2 \end{bmatrix} \tag{B.12}$$

is an indefinite metric tensor. Notice that $\boldsymbol{\eta}$ is a non-canonical Minkowski metric tensor, and also that it is different from the non-canonical Minkowski metric tensor $\mathscr{G}$ defined by Eq. (57).

However, if we consider the following variable transformation:

$$\boldsymbol{\mathscr{y}} = \mathbf{Q}\mathbf{X} \tag{B.13}$$

with

$$\mathbf{Q} = \begin{bmatrix} \mathbf{K}^{1/2} & \mathbf{0}_{n\times 1} \\ \mathbf{0}_{1\times n} & q_y^{-1} \end{bmatrix}, \tag{B.14}$$

from Eqs. (B.8) and (B.10) we can derive Eq. (74) again with

$$\mathbf{A} := \mathbf{Q}^{-1}\mathbf{B}\mathbf{Q} = \frac{1}{q_y}\begin{bmatrix} \mathbf{0}_n & \mathbf{K}^{1/2}\dot{\boldsymbol{\varepsilon}} \\ \dot{\boldsymbol{\varepsilon}}^{\mathrm{t}}\mathbf{K}^{1/2} & 0 \end{bmatrix}. \tag{B.15}$$

The three variables $\boldsymbol{\mathscr{y}}, \boldsymbol{\mathscr{x}}$ and $\mathbf{X}$ have the following relations:

$$\boldsymbol{\mathscr{y}} = \begin{bmatrix} \mathbf{I}_n & \mathbf{K}\mathbf{V} \\ \mathbf{0}_{1\times n} & 1 \end{bmatrix}\boldsymbol{\mathscr{x}} = \mathbf{Q}\mathbf{X}. \tag{B.16}$$

As $\boldsymbol{\mathscr{x}}(t)$ in Eq. (85) we can obtain $\boldsymbol{\mathscr{y}}(t)$ by Eqs. (B.13) and (84),

$$\begin{aligned} \boldsymbol{\mathscr{y}}(t) = &\begin{bmatrix} \mathbf{K}^{1/2} & \mathbf{0}_{1\times n} \\ \mathbf{0}_{1\times n} & q_y^{-1} \end{bmatrix}\begin{bmatrix} \mathbf{G}_s^s(t)(\mathbf{G}_s^s)^{\mathrm{t}}(t_1) - \mathbf{G}_0^s(t)(\mathbf{G}_0^s)^{\mathrm{t}}(t_1) & \mathbf{G}_0^s(t)G_0^0(t_1) - \mathbf{G}_s^s(t)\mathbf{G}_s^0(t_1) \\ \mathbf{G}_s^0(t)(\mathbf{G}_s^s)^{\mathrm{t}}(t_1) - G_0^0(t)(\mathbf{G}_0^s)^{\mathrm{t}}(t_1) & G_0^0(t)G_0^0(t_1) - \mathbf{G}_s^0(t)\mathbf{G}_s^0(t_1) \end{bmatrix} \\ &\times \begin{bmatrix} \mathbf{K}^{-1/2} & \mathbf{0}_{1\times n} \\ \mathbf{0}_{1\times n} & q_y \end{bmatrix}\boldsymbol{\mathscr{y}}(t_1). \end{aligned} \tag{B.17}$$

Then, dividing the first row by the second row of the above solution we can obtain $\boldsymbol{\tau}$ in view of Eq. (B.9), and then $\boldsymbol{\sigma}$ by Eq. (B.2).

## References


Abdel-Karim, M., Ohno, N., 2000. Kinematic hardening model suitable for ratcheting with steady-state. Int. J. Plast. 16, 225–240.

Bari, S., Hassan, T., 2001. Kinematic hardening rules in uncoupled modeling for multiaxial ratcheting simulation. Int. J. Plast. 17, 885–905.

Bari, S., Hassan, T., 2002. An advancement in cyclic plasticity modeling for multiaxial ratcheting simulation. Int. J. Plast. 18, 873–894.

Chaboche, J.L., 1991. On some modifications of kinematic hardening to improve the description of ratcheting effects. Int. J. Plast. 7, 661–678.

Chaboche, J.L., 1994. Modeling of ratcheting: evaluation of various approaches. Eur. J. Mech. A/Solids 13, 501–518.

Chaboche, J.L., Jung, O., 1998. Application of kinematic hardening viscoplasticity model with thresholds to the residual stress relaxation. Int. J. Plast. 13, 785–807.

Corona, E., Hassan, T., Kyriakides, S., 1996. On the performance of kinematic hardening rules in predicting a class of biaxial ratcheting histories. Int. J. Plast. 12, 117–145.

Delobelle, P., Robinet, P., Bocher, L., 1995. Experimental study and phenomenological modelization of ratchet under uniaxial and biaxial loading on an austenitic stainless steel. Int. J. Plast. 11, 295–330.

Drucker, D.C., Prager, W., 1952. Soil mechanics and plastic analysis or limit design. Quart. Appl. Math. 10, 157–165.

Hassan, T., Kyriakides, S., 1992. Ratcheting in cyclic plasticity, Part I: uniaxial behavior, Part II: multiaxial behavior. Int. J. Plast. 8, 91–146.

Hill, R., 1948. A theory of the yielding and plastic flow of anisotropic metals. Proc. Roy. Soc. London A 193, 281–297.

Hong, H.-K., Liu, C.-S., 1999a. Lorentz group $SO_o(5,1)$ for perfect elastoplasticity with large deformation and a consistency numerical scheme. Int. J. Non-Lin. Mech. 34, 1113–1130.

Hong, H.-K., Liu, C.-S., 1999b. Internal symmetry in bilinear elastoplasticity. Int. J. Non-Lin. Mech. 34, 279–288.

Hong, H.-K., Liu, C.-S., 2000. Internal symmetry in the constitutive model of perfect elastoplasticity. Int. J. Non-Lin. Mech. 35, 447–466.

Jiang, Y., Sehitoglu, H., 1994a. Cyclic ratcheting of 1070 steel under multiaxial stress states. Int. J. Plast. 10, 579–608.

Jiang, Y., Sehitoglu, H., 1994b. Multiaxial cyclic ratcheting under multiple step loading. Int. J. Plast. 10, 849–870.

Kang, G., Gao, Q., Yang, X., 2002a. Uniaxial cyclic ratcheting and plastic flow properties of SS304 stainless steel at room and elevated temperatures. Mech. Mater. 34, 145–159.

Kang, G., Gao, Q., 2002. Uniaxial and non-proportionally multiaxial ratcheting of U71Mn rail steel: experiments and simulations. Mech. Mater. 34, 809–820.

Kang, G., Gao, Q., Yang, X., 2002b. A visco-plastic constitutive model incorporated with cyclic hardening for uniaxial/multiaxial ratcheting of SS304 stainless steel at room temperature. Mech. Mater. 34, 521–531.

Kang, G., Gao, Q., Yang, X., 2004. Uniaxial and non-proportionally multiaxial ratcheting of SS304 stainless steel at room temperature: experiments and simulations. Int. J. Non-Lin. Mech. 39, 843–857.

Liu, C., Huang, Y., Stout, M.G., 1997. On the asymmetric yield surface of plastically orthotropic materials: a phenomenological study. Acta Mater. 45, 2397–2406.

Liu, C.-S., 2001a. The *g*-based Jordan algebra and Lie algebra with application to the model of visco-elastoplasticity. J. Marine Sci. Tech. 9, 1–13.

Liu, C.-S., 2001b. Cone of non-linear dynamical system and group preserving schemes. Int. J. Non-Lin. Mech. 36, 1047–1068.

Liu, C.-S., 2003a. Symmetry groups and the pseudo-Riemann spacetimes for mixed-hardening elastoplasticity. Int. J. Solids Struct. 40, 251–269.

Liu, C.-S., 2003b. Smoothing elastoplastic stress–strain curves obtained by a critical modification of conventional models. Int. J. Solids Struct. 40, 2121–2145.

Liu, C.-S., 2004a. A consistent numerical scheme for the von Mises mixed-hardening constitutive equations. Int. J. Plast. 20, 663–704.

Liu, C.-S., 2004b. Lie symmetries of finite strain elastic-perfectly plastic models and exactly consistent schemes for numerical integrations. Int. J. Solids Struct. 41, 1823–1853.

Liu, C.-S., 2004c. Internal symmetry groups for the Drucker–Prager material model of plasticity and numerical integrating methods. Int. J. Solids Struct. 41, 3771–3791.

Liu, C.-S., Chang, C.-W., 2004. Lie group symmetry applied to the computation of convex plasticity constitutive equation. CMES: Comp. Model. Eng. Sci. 6, 277–294.

Liu, C.-S., Hong, H.-K., 2000. The contraction ratios of perfect elastoplasticity under biaxial controls. Eur. J. Mech. A/Solids 19, 827–848.

Liu, C.-S., Hong, H.-K., 2001. Using comparison theorem to compare corotational stress rates in the model of perfect elastoplasticity. Int. J. Solids Struct. 38, 2969–2987.

McDowell, D.L., 1995. Stress state dependence of cyclic ratcheting behavior of two rail steels. Int. J. Plast. 11, 397–421.

Mizuno, M., Mima, Y., Abdel-Karim, M., Ohno, N., 2000. Uniaxial ratcheting of 316FR steel at room temperature—Part I: experiments. J. Eng. Mater. Tech. ASME 122, 29–34.

Mukherjee, S., Liu, C.-S., 2003. Computational isotropic-workhardening rate-independent elastoplasticity. J. Appl. Mech. ASME 70, 644–648.

Ohno, N., Abdel-Karim, M., 2000. Uniaxial ratcheting of 316FR steel at room temperature—Part II: constitutive modeling and simulation. J. Eng. Mater. Tech. ASME 122, 35–41.

Ohno, N., Wang, J.-D., 1993. Kinematic hardening rules with critical state of dynamic recovery, Part I: formulation and basic features for ratcheting behavior, Part II: application to experiments of ratcheting behavior. Int. J. Plast. 9, 375–403.

Ohno, N., Wang, J.-D., 1994. Kinematic hardening rules for simulation of ratcheting behavior. Eur. J. Mech. A/Solids 13, 519–531.

Oller, S., Car, E., Lubliner, J., 2003. Definition of a general implicit orthotropic yield criterion. Comp. Meth. Appl. Mech. Eng. 192, 895–912.

Portier, L., Calloch, S., Marquis, D., Geyer, P., 2000. Ratcheting under tension–torsion loadings: experiments and modelling. Int. J. Plast. 16, 303–335.

Reinicke, K.M., Ralston, T.D., 1977. Plastic limit analysis with an anisotropic, parabolic yield function. Int. J. Rock Mech. Ming Sci. 14, 147–154.

Taheri, S., Lorentz, E., 1999. An elastic–plastic constitutive law for the description of uniaxial and multiaxial ratcheting. Int. J. Plast. 15, 1159–1180.

Voyiadjis, G.Z., Sivakumar, S.M., 1991. A robust kinematic hardening rule with ratcheting effects: Part I. Theoretical formulation. Acta Mech. 90, 105–123.

Voyiadjis, G.Z., Sivakumar, S.M., 1994. A robust kinematic hardening rule with ratcheting effects: Part II. Application to nonproportional loading cases. Acta Mech. 107, 117–136.

Xia, Z., Ellyin, F., 1997. A constitutive model with capability to simulate complex multiaxial ratcheting behaviour of materials. Int. J. Plast. 13, 127–142.

Zhong, W.-X., 1994. Time precise integration method for structural dynamical equations. J. Dalian Univ. Tech. 34, 131–136.